UNIFORM STABILITY FOR LOCAL DISCONTINUOUS GALERKIN METHODS WITH IMPLICIT-EXPLICIT RUNGE-KUTTA TIME DISCRETIZATIONS FOR LINEAR CONVECTION-DIFFUSION EQUATION

HAIJIN WANG, FENGYAN LI, CHI-WANG SHU, AND QIANG ZHANG

ABSTRACT. In this paper, we consider the linear convection-diffusion equation in one dimension with periodic boundary conditions, and analyze the stability of fully discrete methods that are defined with local discontinuous Galerkin (LDG) methods in space and several implicit-explicit (IMEX) Runge-Kutta methods in time. By using the forward temporal differences and backward temporal differences, respectively, we establish two general frameworks of the energy-method based stability analysis. From here, the fully discrete schemes being considered are shown to have monotonicity stability, i.e. the L^2 norm of the numerical solution does not increase in time, under the time step condition $\tau < \mathcal{F}(h/c, d/c^2)$, with the convection coefficient c, the diffusion coefficient d, and the mesh size h. The function \mathcal{F} depends on the specific IMEX temporal method, the polynomial degree k of the discrete space, and the mesh regularity parameter. Moreover, the time step condition becomes $\tau \lesssim h/c$ in the convection-dominated regime and it becomes $\tau \lesssim d/c^2$ in the diffusiondominated regime. The result is improved for a first order IMEX-LDG method. To complement the theoretical analysis, numerical experiments are further carried out, leading to slightly stricter time step conditions that can be used by practitioners. Uniform stability with respect to the strength of the convection and diffusion effects can especially be relevant to guide the choice of time step sizes in practice, e.g. when the convection-diffusion equations are convectiondominated in some sub-regions.

1. Introduction

As a fundamental mathematical model, convection-diffusion equations arise from many science and engineering applications, such as fluid and gas dynamics, semi-conductor device design, meteorology etc. Among the various established numerical methods for such equations, one family is the IMEX-LDG methods, that is defined by following the method-of-lines framework and first applying a local discontinuous Galerkin (LDG) method in space [5]. For the resulted ODE system, an

²⁰¹⁰ Mathematics Subject Classification. Primary 65M12, 65M60.

Key words and phrases. uniform stability, local discontinuous Galerkin method, implicit-explicit time discretization, Runge-Kutta method, convection-diffusion equation.

The first author was supported by NSFC grants 12071214 and 11871428, and Natural Science Research Program for Colleges and Universities of Jiangsu Province grant 20KJB110011.

The second author was supported by NSF grant DMS-1913072.

The third author was supported by NSF grant DMS-2010107 and AFOSR grant FA9550-20-1-0055.

The fourth author is the corresponding author, who was supported by NSFC grant 12071214.

implicit-explicit (IMEX) Runge-Kutta (RK) method is then employed [2, 7], with the convection term treated explicitly and the diffusion term treated implicitly. LDG (and DG) methods have many attractive properties, such as their easy design for arbitrary accuracy, local conservation, flexibility in adaptive implementation, and high parallel efficiency etc. IMEX temporal treatments ensure a good balance of the computational efficiency and numerical stability, and avoid parabolic-type time step restrictions that are often encountered by explicit time integrators for stability due to the stiff diffusion term.

The objective of this paper is to advance the theoretical understanding of IMEX-LDG methods for convection-diffusion equations. Particularly, we consider the one-dimensional linear convection-diffusion equation

(1.1)
$$U_t + cU_x - dU_{xx} = 0, \qquad x \in \Omega = (a, b), \quad t \in (0, T],$$

with the initial condition $U(x,0) = U_0(x)$ and periodic boundary conditions. The nonnegative constants c and d, satisfying $c^2 + d^2 \neq 0$, measure the strength of the convection and the diffusion effects, respectively. In this work, we want to investigate whether numerical stability results can be established *uniformly* with respect to the model parameters c and d for several IMEX-LDG methods solving the equation (1.1).

To motivate our effort and make the objective more precise, we first review some work in literature. In [11], energy-method based stability analysis was performed for three IMEX-LDG methods applied to (1.1) when $d \neq 0$, where the temporal accuracy ranges from first to third order. It shows that these methods are stable, in the sense that the L^2 norm of the numerical solution does not increase in time and hence the methods have monotonicity stability, provided that the time step $\tau \lesssim d/c^2$. Throughout this paper, the notation $X \lesssim Y$ means $X \leq CY$, with C being a positive constant independent of the spatial mesh size h and the term Y. Similar analysis was established in [6, 8, 13] when other DG methods are applied as spatial discretizations. This unconditional-stability type time step condition implies excellent computational efficiency of the methods when d/c^2 is not too small, that is, when the equation (1.1) is relatively in its diffusion-dominated regime.

In the case when d/c^2 is "small" with the convection effect dominating, the time step condition $\tau \lesssim d/c^2$ obtained in [11] is too pessimistic. Intuitively, suitably chosen implicit time discretizations of the diffusion term in the IMEX-LDG methods should not worsen the stability of the methods when they are applied to the diffusion free case with d=0, namely when the explicit RK parts of the temporal schemes are applied to the linear convection (or advection) equation $U_t + cU_x = 0$. Indeed, as established in [17] under a general framework, explicit RK schemes combined with the upwind(-biased) DG spatial discretizations (of certain accuracy) for the linear convection equation have monotonicity stability under the standard hyperbolic CFL condition, namely, $\tau \lesssim h/c$. With the analysis in [17, 11], it is reasonable to expect that certain IMEX-LDG methods for the equation (1.1) have monotonicity stability under a time step condition

(1.2)
$$\tau \le \mathcal{F}(h/c, d/c^2),$$

¹With our assumption on c and d in this paper, one shall interpret both $d/c^2|_{c=0}$ and $hc/d|_{d=0}$ as $+\infty$.

with some function \mathcal{F} , that may depend on the specific IMEX RK method, the polynomial degree for the discrete space, numerical fluxes, and the mesh regularity parameter. It is reasonable to also expect the following two properties:

- Property 1: when $\frac{h/c}{d/c^2} \gg 1$ and the problem is convection-dominated, the condition (1.2) becomes $\tau \lesssim h/c$; Property 2: when $\frac{h/c}{d/c^2} \ll 1$ and the problem is diffusion-dominated, the
- condition (1.2) becomes $\tau \lesssim d/c^2$.

Note that

$$(1.3) P_e := \frac{hc}{d} = \frac{h/c}{d/c^2}$$

is the Péclet mesh number, an important dimensionless quantity for the convectiondiffusion equation (1.1). In this paper, we say an IMEX-LDG method for (1.1) has uniform stability with respect to the model parameters c and d, if it has monotonicity stability under a time step condition as in (1.2) that satisfies Property 1 and Property 2 above. So far, such results are not generally available in theoretical analysis. With our work here, we want to advance the mathematical understanding in this direction by establishing uniform stability for several IMEX-LDG methods for (1.1).

The main theoretical results are obtained through two general frameworks. We first follow the idea of [17] where the explicit Runge-Kutta discontinuous Galerkin (RKDG) methods are analyzed for the convection equation, and establish a general framework of energy analysis starting with a series of forward temporal differences. Energy equations can then be built by using the relationships between these temporal differences and the matrix transferring technique proposed in [17]. with particular attention to the contribution of the numerical discretizations for the diffusion term. In the second framework, the implicit parts of the overall schemes are the focal point of the analysis. We derive energy equations by introducing a series of backward temporal differences and utilizing the relationships between these temporal differences. By combining the stability analysis from these frameworks, the uniform stability results in the form of (1.2) with the two desired properties will naturally follow. The time step condition is further improved for the first order in space and time scheme by better exploring all stabilization mechanisms available.

Uniform stability result as we establish in this work can especially be relevant and informative to guide the choice of time step sizes in practice, e.g. when the convection-diffusion equations are convection-dominated in some sub-regions. Even though the analysis in this paper is performed only for linear convection-diffusion equations, similar stability results can be investigated for more general models, e.g. for convection-diffusion equations with nonlinear convection effect ([12]).

The remainder of the paper is organized as follows. In Section 2, we formulate the semi-discrete in space LDG method, the fully discrete IMEX-LDG schemes, and state the main theoretical results. In Sections 3 and 4, two general frameworks of stability analysis are presented, followed by the analysis for the specific IMEX-LDG methods of our consideration. In Section 5, a more holistic energy-method based stability analysis is performed to improve the result for the first order in space and time scheme. In Section 6, we carry out numerical experiments to complement the theoretical analysis, and this leads to slightly stricter time step conditions one can use in practice. Concluding remarks follow in Section 7.

2. Numerical schemes and main results

In this section, we will start with the semi-discrete LDG scheme in space and review some properties of the spatial discretization. We then present several fully discrete IMEX-LDG methods and state the main theoretical results on numerical stability.

2.1. Semi-discrete in space LDG scheme. We begin with the spatial discretization. Let $Q = \sqrt{d}U_x$, the model (1.1) can be rewritten into its first order form,

(2.1)
$$U_t + cU_x - \sqrt{dQ_x} = 0, \quad Q - \sqrt{dU_x} = 0, \quad x \in \Omega, \quad t \in (0, T].$$

Let $\mathcal{T}_h = \{I_j = (x_{j-\frac{1}{2}}, x_{j+\frac{1}{2}})\}_{j=1}^N$ be the partition of Ω , where $x_{\frac{1}{2}} = a$ and $x_{N+\frac{1}{2}} = b$ are the boundary endpoints. Denote the cell length as $h_j = x_{j+\frac{1}{2}} - x_{j-\frac{1}{2}}$ for $j = 1, \ldots, N$, and define $h = \max_j h_j$. We assume \mathcal{T}_h is quasi-uniform in this paper, that is, there exists a positive constant ρ , referred to as the mesh regularity parameter, such that for all j there holds $h_j/h \geq \rho$ as h goes to zero.

Associated with this mesh, we define the discontinuous finite element space

(2.2)
$$V_h = V_h^k = \{ v \in L^2(\Omega) : v|_{I_j} \in \mathcal{P}_k(I_j), \forall j = 1, \dots, N \},$$

where $\mathcal{P}_k(I_j)$ denotes the space of polynomials in I_j of degree at most $k \geq 0$. Note that the functions in this space are allowed to have discontinuities across element interfaces. For any $v \in V_h$, it has two traces at an element interface $x_{j-\frac{1}{2}}$, namely $v_{j-\frac{1}{2}}^+ = \lim_{\epsilon \to 0^+} v(x_{j-\frac{1}{2}} + \epsilon)$, $v_{j-\frac{1}{2}}^- = \lim_{\epsilon \to 0^-} v(x_{j-\frac{1}{2}} + \epsilon)$, and we denote its jump as $[v]_{j-\frac{1}{2}} = v_{j-\frac{1}{2}}^+ - v_{j-\frac{1}{2}}^-$.

The semi-discrete LDG scheme is the same as that defined in [11]. Let $u(\cdot,0) \in V_h$ be an approximation for the initial data $U_0(x)$ (e.g. via a projection or interpolation), then for any $t \in (0,T]$, find $u(\cdot,t), q(\cdot,t) \in V_h$, such that the following variational forms hold in each cell I_i :

(2.3a)
$$(u_t, v)_j = c\mathcal{H}_j^-(u, v) - \sqrt{d}\mathcal{H}_j^+(q, v), \quad \forall v \in V_h,$$

(2.3b)
$$(q,r)_j = -\sqrt{d}\mathcal{H}_j^-(u,r), \quad \forall r \in V_h.$$

Here $(v,r)_j = \int_{I_j} v(x)r(x)dx$ and

(2.4)
$$\mathcal{H}_{j}^{\pm}(v,r) = (v,r_{x})_{j} - v_{j+\frac{1}{2}}^{\pm} r_{j+\frac{1}{2}}^{-} + v_{j-\frac{1}{2}}^{\pm} r_{j-\frac{1}{2}}^{+},$$

which can be also rewritten as

$$(2.5) \quad \mathcal{H}_{j}^{-}(v,r) = -(v_{x},r)_{j} - [v]_{j-\frac{1}{2}}r_{j-\frac{1}{2}}^{+}, \quad \mathcal{H}_{j}^{+}(v,r) = -(v_{x},r)_{j} - [v]_{j+\frac{1}{2}}r_{j+\frac{1}{2}}^{-}.$$

In the semi-discrete LDG method (2.3), the upwind numerical flux is used for the convective term cU_x , while the alternating numerical flux pair [15] is used for the

diffusive terms $\sqrt{d}U_x$ and $\sqrt{d}Q_x$. Just as in [11], we denote $(\cdot,\cdot) = \sum_{j=1}^{N} (\cdot,\cdot)_j$,

$$\mathcal{H}^{\pm} = \sum_{j=1}^{N} \mathcal{H}_{j}^{\pm}$$
 and

(2.6)
$$\mathcal{H} = c\mathcal{H}^-, \quad \mathcal{L} = -\sqrt{d}\mathcal{H}^+, \quad \text{and} \quad \mathcal{K} = -\sqrt{d}\mathcal{H}^-.$$

Adding up the variational formulations (2.3) over all cells, the semi-discrete LDG scheme becomes: find $u(\cdot,t), q(\cdot,t) \in V_h$, such that

(2.7a)
$$(u_t, v) = \mathcal{H}(u, v) + \mathcal{L}(q, v), \quad \forall v \in V_h,$$

(2.7b)
$$(q, r) = \mathcal{K}(u, r), \quad \forall r \in V_h.$$

When the model (1.1) is diffusion free with d = 0, the LDG scheme becomes the upwind DG method in space for the linear convection (or advection) equation $U_t + cU_x = 0$.

2.2. Properties of the LDG spatial discretization. In this subsection, we will review some standard inverse inequalities for the discrete space V_h and summarize some properties of the LDG spatial discretization. The following notations will be used:

$$\begin{split} \|v\|_j &= \left(\int_{I_j} v^2 dx\right)^{1/2}, \quad \|v\| = \left(\int_{\Omega} v^2 dx\right)^{1/2}, \\ \langle [w], [v] \rangle &= \sum_{j=1}^N [w]_{j-\frac{1}{2}} [v]_{j-\frac{1}{2}}, \quad [\![v]\!]^2 = \langle [v], [v] \rangle = \sum_{j=1}^N [v]_{j-\frac{1}{2}}^2. \end{split}$$

Lemma 2.1. (Inverse inequalities) There exists an inverse constant $\nu = \nu(k)$, such that for any $v \in V_h$

$$(2.8) ||v_x||_j \le \nu h_j^{-1} ||v||_j \le \nu (\rho h)^{-1} ||v||_j,$$

$$(2.9) \max\left\{|v_{j-\frac{1}{2}}^+|,|v_{j+\frac{1}{2}}^-|\right\} \le \sqrt{\nu h_j^{-1}} \|v\|_j \le \sqrt{\nu(\rho h)^{-1}} \|v\|_j.$$

In particular, $\nu(0) = 1$.

One can refer to [1, 10] for these standard inverse inequalities. In the next two lemmas, we recall some properties of the bilinear form \mathcal{H}^{\pm} from [18, 11].

Lemma 2.2. For any $w, v \in V_h$, there hold the following equalities

(2.10a)
$$\mathcal{H}^{\pm}(v,v) = \pm \frac{1}{2} [v]^2,$$

(2.10b)
$$\mathcal{H}^{\pm}(w,v) + \mathcal{H}^{\pm}(v,w) = \pm \langle [w], [v] \rangle,$$

(2.10c)
$$\mathcal{H}^{-}(w,v) = -\mathcal{H}^{+}(v,w).$$

Lemma 2.3. For any $w, v \in V_h$, there hold the following inequalities

(2.11a)
$$|\mathcal{H}^{\pm}(w,v)| \le \left(\|w_x\| + \sqrt{\nu(\rho h)^{-1}} [w]\right) \|v\|,$$

(2.11b)
$$|\mathcal{H}^{\pm}(w,v)| \le \left(\|v_x\| + \sqrt{\nu(\rho h)^{-1}} [v] \right) \|w\|,$$

(2.11c)
$$|\mathcal{H}^{\pm}(w,v)| \le C_{\nu,\rho} h^{-1} ||w|| ||v||.$$

Here $C_{\nu,\rho}$ is a positive constant that is dependent of ν and ρ , and hence dependent of k and ρ .

From Lemmas 2.2 and 2.3, we can immediately get the following corollaries.

Corollary 2.4. Suppose $u, q \in V_h$ satisfy (2.7b), then

$$\mathcal{L}(r,u) = -(q,r), \quad \forall r \in V_h.$$

Particularly,

(2.13)
$$\mathcal{L}(q, u) = -\|q\|^2.$$

Corollary 2.5. Suppose $u, q \in V_h$ satisfy (2.7b), then we have

$$(2.14) ||q|| \le \sqrt{d}C_{\nu,\rho}h^{-1}||u||,$$

where $C_{\nu,\rho}$ is the same as that in Lemma 2.3.

The next lemma establishes an important relationship between the numerical derivative q and the derivative as well as the jump of the numerical solution u, and it plays a vital role in obtaining the unconditional-stability type results as in [11].

Lemma 2.6. [11] Suppose $u, q \in V_h$ satisfy (2.7b) and $d \neq 0$, then there exists a positive constant $\bar{C}_{\nu,\rho}$, dependent of ν and ρ , such that

(2.15)
$$||u_x|| + \sqrt{\nu(\rho h)^{-1}} [\![u]\!] \le \frac{\bar{C}_{\nu,\rho}}{\sqrt{d}} ||q|\!].$$

Furthermore, the property in the following lemma gives some key insight into the stability contribution of the spatial discretization for the convection term.

Lemma 2.7. [17] Let \mathcal{G} be an index set and let $\mathbb{G} = \{g_{ij}\}_{i,j\in\mathcal{G}}$ be a symmetric positive semi-definite matrix. For any $w_i, w_j \in V_h$ with $i, j \in \mathcal{G}$, there holds

(2.16)
$$\sum_{i \in \mathcal{G}} \sum_{j \in \mathcal{G}} g_{ij} \mathcal{H}(w_i, w_j) \leq 0.$$

- 2.3. Fully discrete IMEX(p, r, s)-LDG(k) scheme. For the semi-discrete in space LDG method with the discrete space $V_h = V_h^k$, denoted as LDG(k), we further apply IMEX RK methods in time, denoted as IMEX(p, r, s), to obtain the fully discrete methods. Here s stands for the accuracy order, while p, r are the effective numbers of stages (i.e. the number of function evaluations) of the implicit and explicit parts, respectively. Though there are many options in literature, in this work, we will particularly focus on four methods, IMEX(1,1,1), IMEX(2,2,2), IMEX(4,4,3) and IMEX(3,4,3), with
 - the first three being ARS(1,1,1), ARS (2,2,2), ARS(4,4,3) proposed in [2] with r = p, all being globally stiffly accurate [3] (i.e. with implicit parts being stiffly accurate and explicit parts being FSAL, namely first same as last).
 - the fourth one proposed in [4] with r = p + 1, it is stiffly accurate in the implicit part.

One feature shared by these IMEX RK methods is that, in their standard Butcher tableau representations, the first row and the first column of the matrix for the implicit part are zero. (Such IMEX RK methods are referred to as being of type ARS in [3].) The general framework developed in this paper in Sections 3-4 can be applied to investigate stability of other IMEX RK methods, possibly with additional technical aspects to address for each individual method, as one will see in the upcoming analysis.

With the specific IMEX RK methods mentioned above in mind, we are ready to present our fully discrete methods. Let $\{t^n=n\tau\}_{n=0}^M$ be a uniform mesh over the time interval [0,T], where τ is the time step and $T=t^M$. Let $m=\max\{p,r\}$ and $m_1=\max\{p,r-1\}$. Given the numerical solution $u^n,q^n\in V_h$ at t^n , we seek $u^{n+1},q^{n+1}\in V_h$ at t^{n+1} by the fully discrete IMEX(p,r,s)-LDG(k) scheme as follows:

(S.1) Set
$$u^{n,0} = u^n$$
, $q^{n,0} = q^n$;

(S.2) For
$$\ell = 1, \dots, m$$
, find $u^{n,\ell}, q^{n,\ell} \in V_h$ such that

(2.17a)
$$(u^{n,\ell}, v) = (u^n, v) + \tau \sum_{i=0}^{m_1} \left[c_{\ell i} \mathcal{H}(u^{n,i}, v) + d_{\ell i} \mathcal{L}(q^{n,i}, v) \right], \quad \forall v \in V_h,$$

(2.17b)
$$(q^{n,\ell}, r) = \mathcal{K}(u^{n,\ell}, r), \quad \forall r \in V_h;$$

(S.3) Set
$$u^{n+1} = u^{n,m}$$
, $q^{n+1} = q^{n,m}$.

We list the coefficients of $c_{\ell i}$ and $d_{\ell i}$ below, and one would want to pay attention that the row index ℓ is from 1 to m, and the column index i is from 0 to m_1 . Note that the IMEX RK methods are presented in a slightly different form from the standard ones [2, 4] in order for a more unified analysis. As an example, the final integration step of IMEX(3,4,3) is included in (S.2) instead of (S.3).

IMEX(1,1,1)

$$(2.18) \qquad \frac{c_{\ell i} \quad d_{\ell i}}{1 \quad 0 \quad 0 \quad 1}$$

IMEX(2,2,2)

IMEX(4,4,3)

IMEX(3,4,3)

In (2.19), $\gamma=1-\frac{\sqrt{2}}{2}$ and $\delta=1-\frac{1}{2\gamma}$. In (2.21), θ is the middle root of $6x^3-18x^2+9x-1=0$, which is approximately equal to 0.435866521508459, $\beta_1=-\frac{3}{2}\theta^2+4\theta-\frac{1}{4}$ and $\beta_2=\frac{3}{2}\theta^2-5\theta+\frac{5}{4}$, the parameter α_1 is chosen as $-\frac{1}{4}$ in this paper and $\alpha_2=\frac{\frac{1}{3}-2\theta^2-2\beta_2\alpha_1\theta}{\theta(1-\theta)}$.

- 2.4. **Main stability results.** To make our stability results more precise, we need to specify several notions of numerical stability.
 - i.) Monotonicity stability. There holds $||u^{n+1}|| \le ||u^n||$ for any $n \ge 0$, which implies $||u^n|| \le ||u^0||$.
 - ii.) Exponential-type stability. There holds $||u^{n+1}||^2 \le (1+K\tau)||u^n||^2$ for any $n \ge 0$, where K is a positive constant independent of τ . This implies $||u^n||^2 \le e^{Kt^n}||u^0||^2$.

The concept of the monotonicity stability follows [17], which corresponds to the usual notion of *strong stability*. The next theorem states our main results.

Theorem 2.8. The schemes IMEX(1,1,1)-LDG(0), IMEX(2,2,2)-LDG(k) with k=0,1, IMEX(4,4,3)-LDG(k) and IMEX(3,4,3)-LDG(k) with any integer $k \geq 0$ have monotonicity stability under the time step condition

(2.22a)
$$\tau \leq \max \left\{ \min \left\{ \varrho_1, \varrho_2 P_e \right\} \frac{h}{c}, \varrho_3 \frac{d}{c^2} \right\}$$
(2.22b)
$$= \max \left\{ \min \left\{ \varrho_1, \varrho_2 \frac{h/c}{d/c^2} \right\} \frac{h}{c}, \varrho_3 \frac{d}{c^2} \right\}$$

where $\varrho_1, \varrho_2, \varrho_3$ are positive constants independent of c,d and h, and they depend on the specific IMEX RK method, the polynomial degree k of the discrete space, and the mesh regularity parameter ρ . Furthermore, the condition (2.22) becomes $\tau \leq \varrho_1 h/c$ when d=0, and it is $\tau < +\infty$ and gives unconditional stability when c=0.

Remark 2.9. In Theorem 2.8, the time step condition for the monotonicity stability can be expressed as $\tau \leq \mathcal{F}(h/c,d/c^2)$, where the function \mathcal{F} depends on the specific IMEX RK scheme, the polynomial degree k of the discrete space, and the mesh regularity parameter ρ . Moreover, in the convection-dominated regime with $P_e = \frac{h/c}{d/c^2} \gg 1$, the time step condition becomes $\tau \lesssim h/c$, while in the diffusion-dominated regime with $P_e = \frac{h/c}{d/c^2} \ll 1$, the time step condition becomes $\tau \lesssim d/c^2$. Hence the stability result is uniform with respect to the convection and diffusion coefficients. In the transitional or intermediate regime, the time step condition will depend on both d/c^2 and h/c, as captured by the function \mathcal{F} .

Remark 2.10. For the first order in space and time IMEX(1,1,1)-LDG(0) scheme, the time step condition for the monotonicity stability can be further improved as given in Theorem 5.1 by better exploring all stability mechanisms available.

Remark 2.11. Besides the main results in Theorem 2.8, our analysis also shows that the schemes $\mathrm{IMEX}(1,1,1)\text{-}\mathrm{LDG}(k)$ with $k\geq 1$ and $\mathrm{IMEX}(2,2,2)\text{-}\mathrm{LDG}(k)$ with $k\geq 2$ have monotonicity stability under the time step condition $\tau\lesssim d/c^2$. When the problem is convection-dominated with $P_e=\frac{h/c}{d/c^2}\gg 1$, these methods are stable in a weaker sense (i.e. with an exponential-type stability) under a more stringent time step condition, see Remark 3.6. With the less desirable computational efficiency, these would not be the methods of choice in practice in the convection-dominated regime.

The next two sections will be devoted to the technical details of proving Theorem 2.8, presented through two general frameworks and with the results given in Theorem 3.5 and Theorem 4.3. The first one is based on the forward temporal differences, with the explicit parts of the overall schemes as the focal point of the analysis, while the second one is based on the backward temporal differences, with the implicit parts of the overall schemes as the focal point of the analysis.

3. Stability analysis based on forward temporal differences

At the beginning of this section, we would like to define two CFL numbers

(3.1)
$$\lambda_{\rm c} = c\tau h^{-1}, \qquad \lambda_{\rm d} = d\tau h^{-2}.$$

Throughout this section, we assume $c \neq 0$.

3.1. Energy equation: a general framework. In [17], a general stability analysis framework was established for explicit RKDG methods for the linear convection equation (i.e. (1.1) with d=0), and it will be adapted here to analyze our IMEX-LDG methods, with particular attention to deal with the contribution of the numerical discretizations for the diffusion term.

Following the idea proposed in [17], we define a series of forward temporal differences in the form

$$\mathbb{D}_{\kappa} w^n = \sum_{0 \le \ell \le \kappa} \sigma_{\kappa \ell} w^{n,\ell}, \quad 1 \le \kappa \le m, \quad \text{and} \quad \mathbb{D}_0 w^n = w^n,$$

where w=u,q, such that $\sum_{0\leq\ell\leq\kappa}\sigma_{\kappa\ell}=0,$ and

$$(3.3) \qquad (\mathbb{D}_{\kappa}u^n, v) = \tau \mathcal{H}(\mathbb{D}_{\kappa-1}u^n, v) + \tau \sum_{\ell=0}^{m_1} s_{\kappa\ell} \mathcal{L}(\mathbb{D}_{\ell}q^n, v), \qquad \forall v \in V_h.$$

The coefficients $\{\sigma_{\kappa\ell}\}$ and $\{s_{\kappa\ell}\}$ can be calculated straightforwardly by linear combination of stage evolution in (2.17a) and (3.3). Indeed the calculation process can be conveniently expressed in matrix-vector forms and is summarized as Algorithms 1 and 2. The detail derivation of these algorithms will be put in Appendix A.1.

Algorithm 1. Algorithm for calculating $\{\sigma_{\kappa\ell}\}$:

Step 1. Let $\sigma_{00} = 1$, $\sigma_{0\ell} = 0$ if $\ell \ge 1$.

Denote matrix $A = \{c_{\ell i}\}_{m \times m}$, with $\ell = 1, \ldots, m$ and $i = 0, \ldots, m-1$.

Step 2. For $\kappa = 1, ..., m$, let $\sigma_{\kappa \ell} = 0$ if $\ell > \kappa$. Calculate $\sigma_{\kappa \ell}$ for $\ell = 1...\kappa$ from

$$A_{\kappa}^{\top} \begin{pmatrix} \sigma_{\kappa 1} \\ \vdots \\ \sigma_{\kappa \kappa} \end{pmatrix} = \begin{pmatrix} \sigma_{\kappa - 1, 0} \\ \vdots \\ \sigma_{\kappa - 1, \kappa - 1} \end{pmatrix},$$
 where A_{κ} is the κ -th order leading principal submatrix of A .

Step 3. Let
$$\sigma_{\kappa 0} = -\sum_{1 \le \ell \le m} \sigma_{\kappa \ell}$$
, for $\kappa = 1, \dots, m$.

Algorithm 2. Algorithm for calculating $\{s_{\kappa\ell}\}$:

Step 1. Denote matrix $B = {\sigma_{\ell i}}_{(m_1+1)\times(m_1+1)}$, with $\ell, i = 0, \ldots, m_1$.

Step 2. For $\kappa = 1, \ldots, m$, denote $\hat{m}_{\kappa} = \min\{m_1, \kappa\}$, let $s_{\kappa \ell} = 0$ if $\ell > \hat{m}_{\kappa}$.

For
$$\kappa = 1, ..., m$$
, denote $m_{\kappa} = \min\{m_1, \kappa\}$, let $s_{\kappa\ell} = \text{Calculate } s_{\kappa\ell} \text{ for } \ell = 0, ..., \hat{m}_{\kappa} \text{ from}$

$$B_{\hat{m}_{\kappa}+1}^{\top} \begin{pmatrix} s_{\kappa 0} \\ \vdots \\ s_{\kappa,\hat{m}_{\kappa}} \end{pmatrix} = \sum_{\ell=1}^{\kappa} \sigma_{\kappa\ell} \begin{pmatrix} d_{\ell 0} \\ \vdots \\ d_{\ell,\hat{m}_{\kappa}} \end{pmatrix},$$

where $B_{\hat{m}_{\kappa}+1}$ is the $(\hat{m}_{\kappa}+1)$ -th order leading principal submatrix of B.

Both Algorithm 1 and Algorithm 2 work for the four IMEX schemes (2.18)-(2.21) considered in this paper. It can be verified that, all the leading principal submatrices of A are invertible, and this ensures the existence and uniqueness of the coefficients $\sigma_{\kappa,\ell}$ in Algorithm 1. Particularly, we can obtain that $\sigma_{\kappa,\kappa} \neq 0$ (see Subsection 3.3). In addition, all the leading principal submatrices of B are invertible given B being lower triangular, and this ensures the existence and uniqueness of the coefficients $s_{\kappa\ell}$ in Algorithm 2.

Furthermore, the numerical solution u^{n+1} can be expressed in terms of the forward temporal differences, namely

(3.4)
$$\omega_0 u^{n+1} = \sum_{\ell=0}^m \omega_\ell \mathbb{D}_\ell u^n,$$

where ω_0 is a positive constant, which can be taken as 1 by a proper scaling. Taking L^2 -norm on both sides of (3.4), we get

(3.5)
$$\omega_0^2(\|u^{n+1}\|^2 - \|u^n\|^2) = \sum_{0 \le i, \ell \le m} \omega_{i\ell}(\mathbb{D}_i u^n, \mathbb{D}_\ell u^n) \doteq \mathcal{RHS},$$

where $\omega_{00} = 0$ and $\omega_{i\ell} = \omega_i \omega_\ell$ if $i + \ell > 0$. Note that equation (3.5) alone is not very useful for the stability analysis, because the information of the spatial discretization hence its contribution is not reflected. Similar as in [17], we next will perform a transferring process to convert the inner products of temporal differences in (3.5) into terms of spatial discretizations. This will be accomplished based on the relation (3.3).

To make the idea conveyed more clearly, we first consider the case when d=0. In this case, by using (3.3), we can recursively rewrite \mathcal{RHS} in equation (3.5) as (3.6)

$$\mathcal{RHS} = \mathcal{RHS}(\kappa) = \sum_{0 \le i, \ell \le m} \omega_{i\ell}^{(\kappa)}(\mathbb{D}_i u^n, \mathbb{D}_\ell u^n) + \tau \sum_{0 \le i, \ell \le m} \psi_{i\ell}^{(\kappa)} \mathcal{H}(\mathbb{D}_i u^n, \mathbb{D}_\ell u^n),$$

where the coefficients $\omega_{i\ell}^{(\kappa)}$ and $\psi_{i\ell}^{(\kappa)}$ are obtained by following the matrix transferring procedure introduced in [17] and as outlined below.

For notational convenience, we let $\mathbb{A}^{(\kappa)} = \{\omega_{i\ell}^{(\kappa)}\}$ and $\mathbb{B}^{(\kappa)} = \{\psi_{i\ell}^{(\kappa)}\}$ be symmetric matrices of order m+1, with the initial setting $\mathbb{A}^{(0)} = \{\omega_{i\ell}^{(0)}\} = \{\omega_{i\ell}\}$ and $\mathbb{B}^{(0)} = \mathbb{O}_{m+1}$, and the indices $i, \ell \in \{0, 1, \dots, m\}$. Here and below, we denote by \mathbb{O}_p the zero matrix of order p, and \mathbf{O}_p the zero column vector of dimension p.

With $\kappa \geq 0$, the $(\kappa + 1)$ -th step of the transferring procedure starts from $\mathbb{A}^{(\kappa)}$, with

(3.7)
$$\mathbb{A}^{(\kappa)} = \begin{bmatrix} \mathbb{O}_{\kappa} & \mathbf{0}_{\kappa} & \mathbf{0}_{\kappa} & \cdots & \mathbf{0}_{\kappa} \\ \mathbf{0}_{\kappa}^{\top} & \omega_{\kappa\kappa}^{(\kappa)} & \omega_{\kappa,\kappa+1}^{(\kappa)} & \cdots & \omega_{\kappa m}^{(\kappa)} \\ \mathbf{0}_{\kappa}^{\top} & \omega_{\kappa+1,\kappa}^{(\kappa)} & \omega_{\kappa+1,\kappa+1}^{(\kappa)} & \cdots & \omega_{\kappa+1,m}^{(\kappa)} \\ \vdots & \vdots & \vdots & \ddots & \vdots \\ \mathbf{0}_{\kappa}^{\top} & \omega_{m\kappa}^{(\kappa)} & \omega_{m,\kappa+1}^{(\kappa)} & \cdots & \omega_{mm}^{(\kappa)} \end{bmatrix}.$$

Note that those zeros at the left and the top are null for $\mathbb{A}^{(0)}$. We proceed with two scenarios.

i.) If $\omega_{\kappa\kappa}^{(\kappa)} = 0$, then we get the lower-triangular part of $\mathbb{A}^{(\kappa+1)}$ and $\mathbb{B}^{(\kappa+1)}$ by the following formula

$$(3.8) \qquad \omega_{i\ell}^{(\kappa+1)} = \left\{ \begin{array}{ll} 0, & \ell = \kappa, \\ \omega_{i\ell}^{(\kappa)} - 2\omega_{i+1,\ell-1}^{(\kappa)}, & i = \kappa+1 \text{ and } \ell = \kappa+1, \\ \omega_{i\ell}^{(\kappa)} - \omega_{i+1,\ell-1}^{(\kappa)}, & \kappa+2 \leq i \leq m-1 \text{ and } \ell = \kappa+1, \\ \omega_{i\ell}^{(\kappa)}, & \text{otherwise,} \end{array} \right.$$

and

(3.9)
$$\psi_{i\ell}^{(\kappa+1)} = \begin{cases} 2\omega_{i+1,\ell}^{(\kappa)}, & \kappa \le i \le m-1 \text{ and } \ell = \kappa, \\ \psi_{i\ell}^{(\kappa)}, & \text{otherwise,} \end{cases}$$

which are the same as that given in [17]. In addition, the symmetric property of matrices $\mathbb{A}^{(\kappa+1)}$ and $\mathbb{B}^{(\kappa+1)}$ is preserved in the transferring process. In (3.8), $\omega_{i+1,\ell-1}^{(\kappa)} = 0$ if the index i+1 is greater than m.

ii.) If $\omega_{\kappa\kappa}^{(\kappa)} \neq 0$, we stop the transferring process and define the termination index as $\zeta = \kappa$. With $\omega_{00}^{(0)} = \omega_{00} = 0$, there always holds $\zeta \geq 1$.

Noting the fact that the first ζ rows and columns of $\mathbb{A}^{(\zeta)}$ are zero, and the last row and column of $\mathbb{B}^{(\zeta)}$ are zero, we have at the termination step

$$\mathcal{RHS} = \mathcal{RHS}(\zeta) = \sum_{\zeta \le i, \ell \le m} \omega_{i\ell}^{(\zeta)}(\mathbb{D}_i u^n, \mathbb{D}_\ell u^n) + \sum_{0 \le i, \ell \le m-1} \psi_{i\ell}^{(\zeta)}(\mathbb{D}_{i+1} u^n, \mathbb{D}_\ell u^n)$$

$$(3.10) \qquad \qquad \dot{=} R_1 + R_2,$$

where the term $\tau \mathcal{H}(\mathbb{D}_i u^n, \mathbb{D}_\ell u^n)$ on the right hand side of (3.6) with $\kappa = \zeta$ is written back to $(\mathbb{D}_{i+1}u^n, \mathbb{D}_\ell u^n)$, due to (3.3). Moreover, since the above transferring process is independent of the detailed information of spatial discretization [16], it is easy to see that (3.10) also holds for $d \neq 0$.

The term R_1 can be represented by the matrix $\mathbb{A} \doteq \mathbb{A}^{(\zeta)}$. With the help of the relation (3.3), we express the inner products in R_2 in terms of the discrete spatial operators and get

$$R_{2} = \tau \sum_{0 \leq i, \ell \leq m-1} \psi_{i\ell}^{(\zeta)} \left[\mathcal{H}(\mathbb{D}_{i}u^{n}, \mathbb{D}_{\ell}u^{n}) + \sum_{\varsigma=0}^{m_{1}} s_{i+1,\varsigma} \mathcal{L}(\mathbb{D}_{\varsigma}q^{n}, \mathbb{D}_{\ell}u^{n}) \right]$$

$$= \tau \sum_{0 \leq i, \ell \leq m-1} \psi_{i\ell}^{(\zeta)} \mathcal{H}(\mathbb{D}_{i}u^{n}, \mathbb{D}_{\ell}u^{n}) - \tau \sum_{\ell=0}^{m-1} \sum_{\varsigma=0}^{m_{1}} \phi_{\varsigma\ell}(\mathbb{D}_{\varsigma}q^{n}, \mathbb{D}_{\ell}q^{n})$$

$$\stackrel{\cdot}{=} R_{21} + R_{22},$$

$$(3.11)$$

where we have used (2.12) in the second step with

(3.12)
$$\phi_{\varsigma\ell} = \sum_{i=0}^{m-1} \psi_{i\ell}^{(\varsigma)} s_{i+1,\varsigma}.$$

The term R_{21} can be represented by the matrix $\mathbb{B} \doteq \mathbb{B}^{(\zeta)}$. It is beneficial to represent the term R_{22} in a quadratic form. For this, we define $m_2 = \max\{m-1, m_1\}$, and with zero padding we set $\phi_{\varsigma\ell} = 0$ if $m_1 < \varsigma \le m_2$ or $m-1 < \ell \le m_2$. Furthermore, we define

(3.13)
$$\varphi_{\varsigma\ell} = \varphi_{\ell\varsigma} = \frac{\phi_{\varsigma\ell} + \phi_{\ell\varsigma}}{2},$$

and a symmetric matrix $\mathbb{C} = \{\varphi_{\varsigma\ell}\}$ of order $m_2 + 1$, with indices ς, ℓ from 0 to m_2 , then

(3.14)
$$R_{22} = -\tau \int_{\Omega} \boldsymbol{q}^{n\top} \mathbb{C} \boldsymbol{q}^{n} dx,$$

where $\boldsymbol{q}^n = (\mathbb{D}_0 q^n, \cdots, \mathbb{D}_{m_2} q^n)^{\top}$.

Now we have the energy equation

(3.15)
$$\omega_0^2(\|u^{n+1}\|^2 - \|u^n\|^2) = R_1 + R_{21} + R_{22},$$

with three matrices \mathbb{A} , \mathbb{B} and \mathbb{C} at the termination step. It is important to keep in mind that these matrices only depend on a given IMEX RK method, and particularly \mathbb{A} and \mathbb{B} only depend on the explicit part of the temporal discretization.

3.2. Discussions and general estimate. Now we carry out a general estimate for the terms R_1 , R_{21} and R_{22} , before we turn to more concrete analysis for each fully discrete method in next subsection.

The matrix \mathbb{A} reflects the stability or anti-stability inherited from the temporal discretization, strongly depending on the sign of $\omega_{\zeta\zeta}^{(\zeta)}$. If $\omega_{\zeta\zeta}^{(\zeta)} < 0$, it implies that there is a stability term $-\|\mathbb{D}_{\zeta}u^n\|^2$. Otherwise, if $\omega_{\zeta\zeta}^{(\zeta)} > 0$, it means that there are terms such as $\|\mathbb{D}_{\zeta}u^n\|^2$ with a negative impact on the stability. In either case, using the Cauchy-Schwarz inequality, we have

(3.16)
$$R_1 \le (\omega_{\zeta\zeta}^{(\zeta)} + \varepsilon) \|\mathbb{D}_{\zeta} u^n\|^2 + C_1 \sum_{i=\zeta+1}^m \|\mathbb{D}_i u^n\|^2,$$

where ε is an arbitrary positive constant, C_1 is a positive constant depending on ε and \mathbb{A} .

The matrix \mathbb{B} and \mathbb{C} reflect the contribution of spatial discretizations of the convection part and the diffusion part, respectively. To further investigate such contribution, we follow the idea of [17] to define two contribution indices ρ_c and ρ_d . Specifically, we first define

(3.17)
$$\mathcal{B} = \{ \kappa \colon \det \mathbb{B}_{\kappa+1} \le 0, \text{ and } 0 \le \kappa \le \zeta - 1 \},$$

(3.18)
$$\mathcal{C} = \{ \kappa \colon \det \mathbb{C}_{\kappa+1} \le 0, \text{ and } 0 \le \kappa \le m_2 \},$$

where $\mathbb{B}_{\kappa+1} = \{\psi_{i\ell}^{(\zeta)}\}_{0 \leq i,\ell \leq \kappa}$ and $\mathbb{C}_{\kappa+1} = \{\varphi_{i\ell}\}_{0 \leq i,\ell \leq \kappa}$ are the $(\kappa+1)$ -th order leading principal submatrix of \mathbb{B} and \mathbb{C} , respectively. Then we define

(3.19)
$$\rho_c = \begin{cases} \min\{i : i \in \mathcal{B}\}, & \text{if } \mathcal{B} \neq \emptyset, \\ \zeta, & \text{otherwise,} \end{cases}$$

and

(3.20)
$$\rho_d = \begin{cases} \min\{i : i \in \mathcal{C}\}, & \text{if } \mathcal{C} \neq \emptyset, \\ m_2 + 1, & \text{otherwise.} \end{cases}$$

From the discussions in [16], we know that $\rho_c \geq 1$. Define two sets

(3.21)
$$\pi_1 = \{0, 1, \dots, \rho_c - 1\}, \qquad \pi_2 = \{\rho_c, \rho_c + 1, \dots, m - 1\}.$$

Then we separate R_{21} into

(3.22)
$$R_{21} = \sum_{\xi, \eta = 1, 2} T_{\xi \eta},$$

where

(3.23)
$$T_{\xi\eta} = \tau \sum_{i \in \pi_{\varepsilon}, \ell \in \pi_{n}} \psi_{i\ell}^{(\zeta)} \mathcal{H}(\mathbb{D}_{i}u^{n}, \mathbb{D}_{\ell}u^{n}).$$

Obviously, the submatrix \mathbb{B}_{ρ_c} is positive definite by the definition of (3.19). Thus, $\mathbb{B}_{\rho_c} - \varepsilon_0 \mathbb{I}_{\rho_c}$ is positive semi-definite, where $\varepsilon_0 > 0$ is the smallest eigenvalue of \mathbb{B}_{ρ_c} . Here and below, we denote by \mathbb{I}_p the identity matrix of order p. As a consequence,

(3.24)
$$T_{11} \le -\frac{\varepsilon_0}{2} c \tau \sum_{i \in \pi_1} [\mathbb{D}_i u^n]^2,$$

by Lemma 2.7 and (2.10a). Note that $T_{12} = T_{21} = T_{22} = 0$ when $\pi_2 = \emptyset$. we next consider the general case. With the cardinality of π_i as $\operatorname{card}(\pi_i)$, it is easy to see $\operatorname{card}(\pi_1)\operatorname{card}(\pi_2) \leq m^2/4$. Using (2.10b), Cauchy-Schwarz inequality, the Young's inequality and the inverse inequality (2.9), we get

$$T_{12} + T_{21} = -c\tau \sum_{i \in \pi_1, \ell \in \pi_2} \psi_{i\ell}^{(\zeta)} \langle [\mathbb{D}_i u^n], [\mathbb{D}_\ell u^n] \rangle$$

$$\leq c\tau \max_{i \in \pi_1, \ell \in \pi_2} \{ |\psi_{i\ell}^{(\zeta)}| \} \sum_{i \in \pi_1, \ell \in \pi_2} [\mathbb{D}_i u^n] [\mathbb{D}_\ell u^n]$$

$$\leq \epsilon \varepsilon_0 c\tau \sum_{i \in \pi_1} [\mathbb{D}_i u^n]^2 + \frac{c\tau \operatorname{card}(\pi_1) \operatorname{card}(\pi_2) \max\{ |\psi_{i\ell}^{(\zeta)}|^2 \}}{4\epsilon \varepsilon_0} \sum_{\ell \in \pi_2} [\mathbb{D}_\ell u^n]^2$$

$$\leq \epsilon \varepsilon_0 c\tau \sum_{i \in \pi_1} [\mathbb{D}_i u^n]^2 + \frac{c\tau m^2 \max\{ |\psi_{i\ell}^{(\zeta)}|^2 \} \nu(\rho h)^{-1}}{8\epsilon \varepsilon_0} \sum_{\ell \in \pi_2} ||\mathbb{D}_\ell u^n||^2$$

$$\leq \epsilon \varepsilon_0 c\tau \sum_{i \in \pi_1} [\mathbb{D}_i u^n]^2 + C_2 C_{\nu, \rho} \lambda_c \sum_{\ell \in \pi_2} ||\mathbb{D}_\ell u^n||^2,$$

$$(3.25)$$

where $\epsilon \in (0, \frac{1}{2}]$ is a small positive constant, $C_{\nu,\rho}$ is a positive constant depending on ν and ρ , and C_2 is a positive constant depending on ϵ, ε_0 and the entries of \mathbb{B} , which may have different values in each occurrence. Similarly,

(3.26)
$$T_{22} \le C_2 C_{\nu,\rho} \lambda_c \sum_{\ell \in \pi_2} \| \mathbb{D}_{\ell} u^n \|^2.$$

With all above, we have

$$R_{21} \leq \begin{cases} -(\frac{1}{2} - \epsilon)\varepsilon_0 c\tau \sum_{i=0}^{\rho_c - 1} [\![\mathbb{D}_i u^n]\!]^2 + C_2 C_{\nu,\rho} \lambda_c \sum_{i=\rho_c}^{m-1} \|\mathbb{D}_i u^n \|^2, & \text{if } \pi_2 \neq \emptyset \\ -\frac{\varepsilon_0}{2} c\tau \sum_{i=0}^{\rho_c - 1} [\![\mathbb{D}_i u^n]\!]^2, & \text{otherwise.} \end{cases}$$

If $\rho_d = m_2 + 1$, the matrix \mathbb{C} is positive definite and hence the term R_{22} in (3.14) is nonpositive. This unfortunately is not the case for any IMEX RK scheme in this work, and hence we can not get the stability of the diffusion discretization without any time step restriction in the present analysis framework, as to be seen in next subsection.

To deal with R_{22} , we would like in this paper to add a properly chosen positive number c_0 to its diagonal elements φ_{ii} with $\rho_d \leq i \leq m_2$, so that

(3.28)
$$\mathbb{C}' = \mathbb{C} + c_0 \left[\begin{array}{c} \mathbb{O}_{\rho_d} \\ \mathbb{I}_{m_2+1-\rho_d} \end{array} \right]$$

is positive definite. Furthermore, we take a positive constant c_1 that is not bigger than both c_0 and the smallest (positive) eigenvalue of \mathbb{C}' , and define

(3.29)
$$\mathbb{C}'' = \mathbb{C}' - c_1 \mathbb{I}_{m_2+1} = \mathbb{C} + \left[-\frac{c_1 \mathbb{I}_{\rho_d}}{(c_0 - c_1) \mathbb{I}_{m_2+1-\rho_d}} \right].$$

The resulting matrix \mathbb{C}'' is positive semi-definite. Similar technique was previously used in [11, 6, 13]. Note that the choices of c_0 and c_1 are not unique.

With the help of \mathbb{C}'' , we have

$$R_{22} = -\tau \int_{\Omega} \mathbf{q}^{n\top} \mathbb{C}'' \mathbf{q}^n dx - c_1 \tau \sum_{i=0}^{\rho_d - 1} \|\mathbb{D}_i q^n\|^2 + (c_0 - c_1) \tau \sum_{i=\rho_d}^{m_2} \|\mathbb{D}_i q^n\|^2$$

$$(3.30) \qquad \leq -c_1 \tau \sum_{i=0}^{\rho_d - 1} \|\mathbb{D}_i q^n\|^2 + (c_0 - c_1) C_{\nu,\rho}^2 \lambda_{\mathrm{d}} \sum_{i=\rho_d}^{m_2} \|\mathbb{D}_i u^n\|^2,$$

where Corollary 2.5 was used in the last step, along with the relation $(\mathbb{D}_i q, r) = \mathcal{K}(\mathbb{D}_i u, r)$ for any $r \in V_h$.

Finally, we want to make some remarks on R_1 in (3.16), R_{21} in (3.27), and R_{22} in (3.30). In all these equations, the first term on the right hand side provides stabilization, with the one in (3.16) due to the explicit time discretization if $\omega_{\zeta\zeta}^{(\zeta)}$ is negative, the one in (3.27) due to the upwind discretization of the convection term, and the one in (3.30) due to the dissipation of the diffusion term. And the remaining terms are in the form of multiples of higher order temporal differences of u, with the coefficients at most depending on $C_{\nu,\rho}$, λ_c , λ_d , and they can be potentially controlled by the stabilization terms in these equations under suitable time step condition. We want to point out that the stabilization mechanism provided by the implicit treatment of the diffusion term is not fully utilized in the current framework, and this will be further explored in Section 4.

- 3.3. Four specific applications. We are now ready to apply the general analysis built so far to examine the stability of specific IMEX-LDG schemes, including IMEX(1,1,1)-LDG(k), IMEX(2,2,2)-LDG(k), IMEX(4,4,3)-LDG(k), IMEX(3,4,3)-LDG(k), with k as any nonnegative integer.
- 3.3.1. IMEX(1,1,1)-LDG(k). For the first order in time IMEX(1,1,1)-LDG(k) scheme in (2.17)-(2.18), $m=m_1=m_2=1$. It is easy to see that $\mathbb{D}_1u^n=u^{n+1}-u^n$, $s_{10}=s_{11}=1$, and $u^{n+1}=\mathbb{D}_0u^n+\mathbb{D}_1u^n$. Thus

$$\mathbb{A}^{(0)} = \begin{bmatrix} 0 & 1 \\ 1 & 1 \end{bmatrix}, \quad \mathbb{B}^{(0)} = \mathbb{O}.$$

By the matrix transferring formulas (3.8) and (3.9), we have

$$\mathbb{A}^{(1)} = \begin{bmatrix} 0 & \vdots \\ 0 & 1 \end{bmatrix}, \quad \mathbb{B}^{(1)} = \begin{bmatrix} 2 & 0 \\ 0 & 0 \end{bmatrix}.$$

Note that $\omega_{11}^{(1)}=1>0$, the transferring process is terminated here, with $\zeta=1$, $\mathbb{A}=\mathbb{A}^{(1)}$ and $\mathbb{B}=\mathbb{B}^{(1)}$. Moreover, we have

(3.31)
$$\mathbb{C} = \begin{bmatrix} 2 & 1 \\ 1 & 0 \end{bmatrix}.$$

One can check that the contribution indices $\rho_c = \rho_d = 1$. Taking $c_0 = 2, c_1 = 1$ in (3.29), we get

$$(3.32) \mathcal{RHS} \le -c\tau \|\mathbb{D}_0 u^n\|^2 - \tau \|\mathbb{D}_0 q^n\|^2 + (1 + C_{\nu,\rho}^2 \lambda_{\mathrm{d}}) \|\mathbb{D}_1 u^n\|^2.$$

The estimate for $\|\mathbb{D}_1 u^n\|^2$ is given in the next lemma, whose proof is put in Appendix A.2.

Lemma 3.1. When $k \geq 1$, we have

(3.33)
$$\|\mathbb{D}_1 u^n\|^2 \le C_{\nu,\rho}^2 \lambda_c^2 \|\mathbb{D}_0 u^n\|^2 + \frac{\tau}{2} \|\mathbb{D}_0 q^n\|^2.$$

For the special case k = 0, we have

(3.34)
$$\|\mathbb{D}_1 u^n\|^2 \le c\tau C_{\nu,\rho} \lambda_c [\![\mathbb{D}_0 u^n]\!]^2 + \frac{\tau}{2} \|\mathbb{D}_0 q^n\|^2.$$

The stability of the IMEX(1,1,1)-LDG(k) scheme can be stated as two cases:

Case 1: $k \ge 1$. Substituting (3.33) into (3.32), we can get the exponential-type stability if

(3.35)
$$\begin{cases} \frac{1}{2} \left(1 + C_{\nu,\rho}^2 \lambda_{\rm d} \right) \leq 1, \\ C_{\nu,\rho}^2 \lambda_{\rm c}^2 \leq \hat{C}\tau, & \text{for any positive constant } \hat{C}, \end{cases}$$

(3.36)
$$\lambda_{\rm c}^2 \le \frac{\hat{C}\tau}{C_{\nu,o}^2}, \quad \lambda_{\rm d} \le \frac{1}{C_{\nu,o}^2}.$$

This, with $d = ch/P_e$, is equivalent to the following time step condition

<u>Case 2: k = 0.</u> Substituting (3.34) into (3.32), we can get the monotonicity stability if

(3.38)
$$\begin{cases} \frac{1}{2} \left(1 + C_{\nu,\rho}^2 \lambda_{\rm d} \right) \le 1, \\ C_{\nu,\rho} \lambda_{\rm c} \le \frac{1}{2}, \end{cases}$$

namely,

(3.39)
$$\lambda_{\rm c} \le \frac{1}{2C_{\nu,\rho}}, \quad \lambda_{\rm d} \le \frac{1}{C_{\nu,\rho}^2}.$$

This is equivalent to the following time step condition

(3.40)
$$\tau \le \min \left\{ \frac{1}{2C_{\nu,\rho}}, \frac{P_e}{C_{\nu,\rho}^2} \right\} \frac{h}{c}.$$

3.3.2. IMEX(2,2,2)-LDG(k). For the second order in time IMEX(2,2,2)-LDG(k) scheme in (2.17) and (2.19), $m=m_1=m_2=2$. By Algorithm 1 and Algorithm 2, we can get

$$\begin{bmatrix} \mathbb{D}_0 u^n \\ \mathbb{D}_1 u^n \\ \mathbb{D}_2 u^n \end{bmatrix} = \begin{bmatrix} 1 \\ -\frac{1}{\gamma} & \frac{1}{\gamma} \\ \frac{2}{\gamma} - 2 & -\frac{2}{\gamma} & 2 \end{bmatrix} \begin{bmatrix} u^n \\ u^{n,1} \\ u^{n+1} \end{bmatrix},$$

(3.42)
$$s_{10} = 1, \quad s_{11} = \gamma, \qquad s_{12} = 0, s_{20} = 0, \quad s_{21} = 2\gamma(1 - \gamma), \quad s_{22} = \gamma.$$

It is easy to check that

$$(3.43) 2u^{n+1} = 2\mathbb{D}_0 u^n + 2\mathbb{D}_1 u^n + \mathbb{D}_2 u^n.$$

Hence, the initial energy equation can be expressed by the matrices

$$\mathbb{A}^{(0)} = \begin{bmatrix} 0 & 4 & 2 \\ 4 & 4 & 2 \\ 2 & 2 & 1 \end{bmatrix}, \quad \mathbb{B}^{(0)} = \mathbb{O},$$

which are the same as that given in [17] for the second order RKDG scheme. The matrix transferring procedure is also the same as that in [17], leading to

$$\mathbb{A}^{(1)} = \begin{bmatrix} 0 & & & \\ & 0 & 2 \\ & 2 & 1 \end{bmatrix}, \quad \mathbb{B}^{(1)} = \begin{bmatrix} 8 & 4 & 0 \\ 4 & 0 & 0 \\ 0 & 0 & 0 \end{bmatrix},$$

(3.44)
$$\mathbb{A}^{(2)} = \begin{bmatrix} 0 & & \\ & 0 & \\ & & 1 \end{bmatrix}, \quad \mathbb{B}^{(2)} = \begin{bmatrix} 8 & 4 & 0 \\ 4 & 4 & 0 \\ \hline 0 & 0 & 0 \end{bmatrix}.$$

Since $\omega_{22}^{(2)}=1>0$, we stop the transferring and get $\zeta=2$. Therefore, $\mathbb{A}=\mathbb{A}^{(2)}$ and $\mathbb{B}=\mathbb{B}^{(2)}$. Moreover, from (3.12) and (3.13), one can obtain

(3.45)
$$\mathbb{C} = \begin{bmatrix} 8 & 2 + 8\gamma - 4\gamma^2 & 2\gamma \\ 2 + 8\gamma - 4\gamma^2 & 12\gamma - 8\gamma^2 & 2\gamma \\ 2\gamma & 2\gamma & 0 \end{bmatrix}.$$

We can check that the contribution indices $\rho_c = \rho_d = 2$. Taking $c_0 = 1, c_1 = \frac{1}{2}$ in (3.29), we can get (3.46)

$$\mathcal{RHS} \leq -\frac{\varepsilon_0}{2}c\tau([\![\mathbb{D}_0u^n]\!]^2 + [\![\mathbb{D}_1u^n]\!]^2) - \frac{\tau}{2}(|\![\mathbb{D}_0q^n]\!]^2 + |\![\mathbb{D}_1q^n]\!]^2) + \left(1 + \frac{C_{\nu,\rho}^2\lambda_{\mathrm{d}}}{2}\right) |\![\mathbb{D}_2u^n]\!]^2,$$

where $\varepsilon_0 = 6 - 2\sqrt{5}$. The estimate for $\|\mathbb{D}_2 u^n\|^2$ is given in the next lemma, whose proof is put in Appendix A.3.

Lemma 3.2. When $k \geq 2$, we have

$$(3.47) \|\mathbb{D}_2 u^n\|^2 \le C_{\nu,\rho}^4 \lambda_c^4 \|\mathbb{D}_0 u^n\|^2 + \frac{C_{\nu,\rho}^2 \lambda_c^2 \tau}{2\gamma} \|\mathbb{D}_0 q^n\|^2 + \gamma \tau \|\mathbb{D}_1 q^n\|^2.$$

For the case $k \leq 1$, we have

$$\|\mathbb{D}_{2}u^{n}\|^{2} \leq 4c\tau [(C_{\nu,\rho}\lambda_{c})^{3} \|\mathbb{D}_{0}u^{n}\|^{2} + C_{\nu,\rho}\lambda_{c} \|\mathbb{D}_{1}u^{n}\|^{2}]$$

$$+ 4C_{\nu,\rho}^{4}\lambda_{c}^{2}\lambda_{d}\tau(\gamma\|\mathbb{D}_{1}q^{n}\|^{2} + \|\mathbb{D}_{0}q^{n}\|^{2}) + \gamma\tau\|\mathbb{D}_{1}q^{n}\|^{2}.$$
(3.48)

Remark 3.3. For the case $k \leq 1$, $\|\mathbb{D}_2 u^n\|$ can be bounded by the "good terms" provided by all the stabilization mechanisms, i.e. due to the upwind spatial discretization of the convection part and the implicit temporal discretization of the diffusion part. This is an improvement over that for the case $k \geq 2$, and thus monotonicity stability can be obtained under the time step condition $\tau \lesssim h/c$, as to be shown next.

Similar comment goes to the case k=0 in the previous subsection. Indeed, such improved performance of the first and second order in time methods with

lower degree polynomials in space is an important property of fully discrete DG methods, as previously shown for the pure convection equation (with d = 0) in [17].

In what follows we present the stability results for the IMEX(2,2,2)-LDG(k) scheme as two cases:

Case 1: $k \geq 2$. Substituting (3.47) into (3.46), we get

(3.49)
$$\mathcal{RHS} \leq \left(1 + \frac{C_{\nu,\rho}^2}{2} \lambda_{\mathrm{d}}\right) C_{\nu,\rho}^4 \lambda_{\mathrm{c}}^4 \|u^n\|^2,$$

if

$$(3.50) \qquad \left(1 + \frac{C_{\nu,\rho}^2}{2} \lambda_{\rm d}\right) \max \left\{\frac{C_{\nu,\rho}^2 \lambda_{\rm c}^2}{2\gamma}, \gamma\right\} \le \frac{1}{2},$$

which can be fulfilled by letting

(3.51)
$$\lambda_{\rm c} \leq \frac{\sqrt{2}\gamma}{C_{\nu,\rho}} \quad \text{and} \quad \lambda_{\rm d} \leq \frac{1-2\gamma}{\gamma C_{\nu,\rho}^2}.$$

To further control (3.49), we impose

$$(3.52) C_{\nu,\rho}^4 \lambda_{\rm c}^4 \le \hat{C}\tau,$$

with any given positive constant \hat{C} . Under the above conditions we will have exponential-type stability. Noting that $d = ch/P_e$, then the conditions (3.51)-(3.52) altogether require

(3.53)
$$\tau \leq \min \left\{ \frac{\sqrt{2}\gamma}{C_{\nu,\rho}} \frac{h}{c}, \frac{(1-2\gamma)P_e}{\gamma C_{\nu,\rho}^2} \frac{h}{c}, \frac{\hat{C}^{1/3}}{C_{\nu,\rho}^{4/3}} \left(\frac{h}{c}\right)^{4/3} \right\}.$$

Case 2: $k \le 1$. Substituting (3.48) into (3.46), we can get monotonicity stability if

$$(3.54) \qquad \begin{cases} 4\left(1 + \frac{C_{\nu,\rho}^2}{2}\lambda_{\mathrm{d}}\right) \max\left\{(C_{\nu,\rho}\lambda_{\mathrm{c}})^3, C_{\nu,\rho}\lambda_{\mathrm{c}}\right\} \leq \frac{\varepsilon_0}{2}, \\ \left(1 + \frac{C_{\nu,\rho}^2}{2}\lambda_{\mathrm{d}}\right) \max\left\{4C_{\nu,\rho}^4\lambda_{\mathrm{c}}^2\lambda_{\mathrm{d}}, 4C_{\nu,\rho}^4\lambda_{\mathrm{c}}^2\lambda_{\mathrm{d}}\gamma + \gamma\right\} \leq \frac{1}{2}, \end{cases}$$

where $\varepsilon_0 = 6 - 2\sqrt{5}$. This condition can be fulfilled by letting

(3.55)
$$\begin{cases} \lambda_{c} \leq \min \left\{ \frac{1}{C_{\nu,\rho}}, \frac{\varepsilon_{0}\gamma}{4(1-\gamma)C_{\nu,\rho}} \right\}, \\ \lambda_{d} \leq \min \left\{ \frac{\gamma}{4(1-\gamma)C_{\nu,\rho}^{2}}, \frac{1-3\gamma}{\gamma C_{\nu,\rho}^{2}} \right\}. \end{cases}$$

Noting that $d = ch/P_e$, then condition (3.55) becomes

(3.56)
$$\tau \leq \min \left\{ \frac{(6 - 2\sqrt{5})\gamma}{4(1 - \gamma)C_{\nu,\rho}}, \frac{\gamma P_e}{4(1 - \gamma)C_{\nu,\rho}^2} \right\} \frac{h}{c}.$$

3.3.3. IMEX(4,4,3)-LDG(k). For the third order in time IMEX(4,4,3)-LDG(k) scheme in (2.17) and (2.20), $m=m_1=m_2=4$. We have

$$(3.57) \qquad \begin{bmatrix} \mathbb{D}_0 u^n \\ \mathbb{D}_1 u^n \\ \mathbb{D}_2 u^n \\ \mathbb{D}_3 u^n \\ \mathbb{D}_4 u^n \end{bmatrix} = \begin{bmatrix} 1 \\ -2 & 2 \\ 12 & -48 & 36 \\ 72 & -360 & 216 & 72 \\ \frac{4896}{7} & -\frac{23616}{7} & \frac{15552}{7} & \frac{3456}{7} & -\frac{288}{7} \end{bmatrix} \begin{bmatrix} u^n \\ u^{n,1} \\ u^{n,2} \\ u^{n,3} \\ u^{n+1} \end{bmatrix}.$$

The coefficients $s_{\ell i}$ are given as

It can be verified that

(3.59)
$$u^{n+1} = u^n + \sum_{\ell=1}^{4} \omega_{\ell} \mathbb{D}_{\ell} u^n,$$

where

(3.60)
$$\omega_1 = 1, \quad \omega_2 = \frac{1}{2}, \quad \omega_3 = \frac{1}{6}, \quad \omega_4 = -\frac{7}{288}.$$

Hence, the initial energy equation can be expressed by the matrices

$$\mathbb{A}^{(0)} = \begin{bmatrix} 0 & 1 & \frac{1}{2} & \frac{1}{6} & -\frac{7}{288} \\ 1 & 1 & \frac{1}{2} & \frac{1}{6} & -\frac{7}{288} \\ \frac{1}{2} & \frac{1}{2} & \frac{1}{4} & \frac{1}{12} & -\frac{7}{576} \\ \frac{1}{67} & -\frac{1}{7288} & -\frac{7}{776} & -\frac{1728}{1728} & \frac{49}{82944} \end{bmatrix}, \quad \mathbb{B}^{(0)} = \mathbb{O}.$$

Since $\omega_{00}^{(0)} = 0$, we carry out the transferring process and get

$$\mathbb{A}^{(1)} = \begin{bmatrix} 0 & & & & & \\ & 0 & \frac{1}{3} & \frac{55}{288} & -\frac{7}{288} \\ & \frac{1}{3} & \frac{1}{4} & \frac{1}{12} & -\frac{7}{576} \\ & \frac{55}{288} & \frac{1}{12} & \frac{36}{6} & -\frac{7}{1728} \\ & -\frac{7}{288} & -\frac{7}{576} & -\frac{7}{1728} & \frac{49}{82944} \end{bmatrix}, \quad \mathbb{B}^{(1)} = \begin{bmatrix} 2 & 1 & \frac{1}{3} & -\frac{7}{144} & 0 \\ 1 & 0 & 0 & 0 & 0 \\ \frac{1}{3} & 0 & 0 & 0 & 0 \\ -\frac{7}{144} & 0 & 0 & 0 & 0 \\ 0 & 0 & 0 & 0 & 0 \end{bmatrix}.$$

Noting that $\omega_{11}^{(1)} = 0$, so we continue the transferring and get

$$\mathbb{A}^{(2)} = \begin{bmatrix} 0 & & & & & \\ & 0 & & & & \\ & & -\frac{19}{144} & \frac{31}{288} & -\frac{7}{576} \\ \frac{31}{288} & \frac{1}{36} & -\frac{7}{1728} \\ -\frac{7}{576} & -\frac{7}{1728} & \frac{82944}{82944} \end{bmatrix}, \quad \mathbb{B}^{(2)} = \begin{bmatrix} 2 & 1 & \frac{1}{3} & -\frac{7}{144} & 0 \\ 1 & \frac{2}{3} & \frac{55}{144} & -\frac{7}{144} & 0 \\ -\frac{1}{3} & \frac{55}{144} & 0 & 0 & 0 \\ -\frac{7}{144} & -\frac{7}{144} & 0 & 0 & 0 \\ 0 & 0 & 0 & 0 & 0 \end{bmatrix}.$$

Since $\omega_{22}^{(2)} < 0$, we stop the transferring and get $\zeta = 2$. Therefore, $\mathbb{A} = \mathbb{A}^{(2)}$ and $\mathbb{B} = \mathbb{B}^{(2)}$. In addition, we can calculate those coefficients $\varphi_{\varsigma\ell}$ from (3.12) and (3.13) and yield

(3.61)
$$\mathbb{C} = \begin{bmatrix} 2 & 1 & \frac{1}{3} & \frac{19}{288} & -\frac{7}{576} \\ 1 & \frac{2}{3} & \frac{55}{72} & \frac{55}{722} & \frac{5}{288} & -\frac{7}{576} \\ \frac{1}{3} & \frac{55}{72} & \frac{55}{288} & -\frac{7}{576} & 0 \\ \frac{19}{288} & \frac{58}{756} & -\frac{7}{576} & 0 & 0 \\ -\frac{7}{576} & -\frac{7}{576} & 0 & 0 & 0 \end{bmatrix}.$$

One can check that $\rho_c = \rho_d = 2$. Taking $c_0 = 10, c_1 = \frac{1}{10}$ in (3.29), we can get

$$\mathcal{RHS} \leq -\left(\frac{1}{2} - \epsilon\right)\varepsilon_{0}(\|\mathbb{D}_{0}u^{n}\|^{2} + \|\mathbb{D}_{1}u^{n}\|^{2}) - \frac{\tau}{10}(\|\mathbb{D}_{0}q^{n}\|^{2} + \|\mathbb{D}_{1}q^{n}\|^{2}) - (\frac{19}{144} - \varepsilon)\|\mathbb{D}_{2}u^{n}\|^{2} + C_{1}(\|\mathbb{D}_{3}u^{n}\|^{2} + \|\mathbb{D}_{4}u^{n}\|^{2}) + C_{2}C_{\nu,\rho}\lambda_{c}(\|\mathbb{D}_{2}u^{n}\|^{2} + \|\mathbb{D}_{3}u^{n}\|^{2})$$

(3.62)
$$+ \frac{99}{10} C_{\nu,\rho}^2 \lambda_{\mathrm{d}} (\|\mathbb{D}_2 u^n\|^2 + \|\mathbb{D}_3 u^n\|^2 + \|\mathbb{D}_4 u^n\|^2),$$

for any positive ϵ and ε , where $\varepsilon_0 = \frac{4-\sqrt{13}}{3}$, C_1 and C_2 are positive constants depending on ε and ϵ , respectively. Taking $\epsilon = \frac{1}{2}$ and $\varepsilon = \frac{4}{144}$, we have

$$\mathcal{RHS} \leq \left(-\frac{15}{144} + C_2 C_{\nu,\rho} \lambda_{c} + 10 C_{\nu,\rho}^2 \lambda_{d} \right) \| \mathbb{D}_2 u^n \|^2 - \frac{\tau}{10} (\| \mathbb{D}_0 q^n \|^2 + \| \mathbb{D}_1 q^n \|^2)$$

$$(3.63) \qquad + \left(C_1 + C_2 C_{\nu,\rho} \lambda_{c} + 10 C_{\nu,\rho}^2 \lambda_{d} \right) (\| \mathbb{D}_3 u^n \|^2 + \| \mathbb{D}_4 u^n \|^2).$$

Lemma 3.4. The forward temporal differences $\mathbb{D}_3 u^n$ and $\mathbb{D}_4 u^n$ defined in (3.57) satisfy

where

$$\begin{aligned} \mathcal{Q}_{31} &= 2C_{\nu,\rho}^2 \lambda_{\rm c}^2 + 4s_{32}^2 C_{\nu,\rho}^4 \lambda_{\rm d}^2; & \mathcal{Q}_{41} &= (2C_{\nu,\rho}^2 \lambda_{\rm c}^2 + 6s_{43}^2 C_{\nu,\rho}^4 \lambda_{\rm d}^2) \mathcal{Q}_{31} + 6s_{42}^2 C_{\nu,\rho}^4 \lambda_{\rm d}^2; \\ \mathcal{Q}_{32} &= 4s_{31}^2 C_{\nu,\rho}^2 \lambda_{\rm d}; & \mathcal{Q}_{42} &= (2C_{\nu,\rho}^2 \lambda_{\rm c}^2 + 6s_{43}^2 C_{\nu,\rho}^4 \lambda_{\rm d}^2) \mathcal{Q}_{32} + 6s_{41}^2 C_{\nu,\rho}^2 \lambda_{\rm d}, \end{aligned}$$

with the coefficients $s_{\ell i}$ given in (3.58).

The proof of this lemma is put in Appendix A.4. Owing to Lemma 3.4, we have

$$\mathcal{RHS} \leq -\frac{15}{144} \|\mathbb{D}_{2}u^{n}\|^{2} - \frac{\tau}{10} (\|\mathbb{D}_{0}q^{n}\|^{2} + \|\mathbb{D}_{1}q^{n}\|^{2})$$

$$+ \mathcal{Q}_{1}(\lambda_{c}, \lambda_{d}) \|\mathbb{D}_{2}u^{n}\|^{2} + \mathcal{Q}_{2}(\lambda_{c}, \lambda_{d})\tau \|\mathbb{D}_{1}q^{n}\|^{2}$$

$$(3.65)$$

where

$$\begin{aligned} \mathcal{Q}_{1}(\lambda_{\rm c},\lambda_{\rm d}) &= (C_{1} + C_{2}C_{\nu,\rho}\lambda_{\rm c} + 10C_{\nu,\rho}^{2}\lambda_{\rm d})(\mathcal{Q}_{31} + \mathcal{Q}_{41}) + (C_{2}C_{\nu,\rho}\lambda_{\rm c} + 10C_{\nu,\rho}^{2}\lambda_{\rm d}), \\ \mathcal{Q}_{2}(\lambda_{\rm c},\lambda_{\rm d}) &= (C_{1} + C_{2}C_{\nu,\rho}\lambda_{\rm c} + 10C_{\nu,\rho}^{2}\lambda_{\rm d})(\mathcal{Q}_{32} + \mathcal{Q}_{42}). \end{aligned}$$

Hence, if

(3.66)
$$Q_1(\lambda_c, \lambda_d) \le \frac{15}{144} \text{ and } Q_2(\lambda_c, \lambda_d) \le \frac{1}{10},$$

then we can get the monotonicity stability.

The conditions in (3.66) can be fulfilled by letting λ_c and λ_d be smaller than ϱ_1 and ϱ_2 , respectively, with ϱ_1 and ϱ_2 as positive constants depending on C_1 , C_2 and $C_{\nu,\rho}$ and hence on k and ρ . This, in combination with $d = ch/P_e$, leads to the following time step restriction for stability

(3.67)
$$\tau \le \min\{\varrho_1, \varrho_2 P_e\} \frac{h}{c}.$$

3.3.4. IMEX(3,4,3)-LDG(k). The analysis for the third order in time IMEX(3,4,3)-LDG(k) scheme in (2.17) and (2.21) is similar to that for the IMEX(4,4,3)-LDG(k) scheme. So we will mainly highlight the differences. For the IMEX(3,4,3)-LDG(k) scheme, $m=4, m_1=m_2=3$. With the definition

$$(3.68) \begin{bmatrix} \mathbb{D}_0 u^n \\ \mathbb{D}_1 u^n \\ \mathbb{D}_2 u^n \\ \mathbb{D}_3 u^n \\ \mathbb{D}_4 u^n \end{bmatrix} = \begin{bmatrix} \sigma_{00} & & & & \\ \sigma_{10} & \sigma_{11} & & & \\ \sigma_{20} & \sigma_{21} & \sigma_{22} & & & \\ \sigma_{30} & \sigma_{31} & \sigma_{32} & \sigma_{33} & & \\ \sigma_{40} & \sigma_{41} & \sigma_{42} & \sigma_{43} & \sigma_{44} \end{bmatrix} \begin{bmatrix} u^n \\ u^{n,1} \\ u^{n,2} \\ u^{n,3} \\ u^{n+1} \end{bmatrix},$$

where the coefficients $\sigma_{\kappa\ell}$ are listed in Appendix A.5, and the relationship (3.59) holds with

(3.69)
$$\omega_1 = 1, \quad \omega_2 = \frac{1}{2}, \quad \omega_3 = \frac{1}{6}, \quad \omega_4 = \alpha_1 \alpha_2 \theta^2.$$

Similar as for the IMEX(4,4,3)-LDG(k) scheme, we carry out the transferring procedure and obtain,

$$\mathbb{A}^{(2)} = \begin{bmatrix} 0 & & & & & & \\ & 0 & & & & & \\ & & & 2\alpha_1\alpha_2\theta^2 - \frac{1}{12} & \frac{1}{12} - \alpha_1\alpha_2\theta^2 & \frac{1}{2}\alpha_1\alpha_2\theta^2 \\ & & \frac{1}{12} - \alpha_1\alpha_2\theta^2 & & \frac{1}{36} & \frac{1}{6}\alpha_1\alpha_2\theta^2 \\ & & \frac{1}{2}\alpha_1\alpha_2\theta^2 & & \frac{1}{6}\alpha_1\alpha_2\theta^2 & \alpha_1^2\alpha_2^2\theta^4 \end{bmatrix},$$

$$\mathbb{B}^{(2)} = \begin{bmatrix} 2 & 1 & \frac{1}{3} & 2\alpha_1\alpha_2\theta^2 & 0\\ 1 & \frac{2}{3} & \frac{1}{3} - 2\alpha_1\alpha_2\theta^2 & \frac{1}{3} - 2\alpha_1\alpha_2\theta^2 & 0\\ \frac{1}{3} & \frac{1}{3} - 2\alpha_1\alpha_2\theta^2 & 0 & 0 & 0\\ 2\alpha_1\alpha_2\theta^2 & 2\alpha_1\alpha_2\theta^2 & 0 & 0 & 0\\ 0 & 0 & 0 & 0 & 0 \end{bmatrix}.$$

We can verify that $\omega_{22}^{(2)} = 2\alpha_1\alpha_2\theta^2 - \frac{1}{12} < 0$ if $\alpha_1 \in (-0.27, 0.35)$. Our specific choice $\alpha_1 = -\frac{1}{4}$ falls into this range, hence the transferring is terminated with $\zeta = 2$, $\mathbb{A} = \mathbb{A}^{(2)}$ and $\mathbb{B} = \mathbb{B}^{(2)}$. In addition, we can calculate those coefficients $\varphi_{\varsigma\ell}$ from (3.12) and (3.13), and yield

(3.70)
$$\mathbb{C} = \begin{bmatrix} 2 & 1 & \frac{1}{3} & \varphi_{03} \\ \frac{1}{3} & \frac{2}{3} & \frac{\varphi_{12}}{\varphi_{22}} & \frac{\varphi_{13}}{\varphi_{23}} \\ \frac{\varphi_{03}}{\varphi_{03}} & \varphi_{13} & \varphi_{23} & 0 \end{bmatrix},$$

where $\varphi_{03} = \frac{\alpha_1 \theta s_*}{3(\theta - 1)}$ with $s_* = 18 \alpha_1 \theta^3 - 60 \alpha_1 \theta^2 + 15 \alpha_1 \theta + 12 \theta^2 - 2$, $\varphi_{12} = \frac{1}{24\alpha_1} (18 \alpha_1 \theta^4 - 30 \alpha_1 \theta^3 + 27 \alpha_1 \theta^2 - 7 \alpha_1 \theta + 4 \alpha_1 - 2 \theta + 2)$, $\varphi_{13} = \frac{\theta(2\alpha_1 - \theta + 1)s_*}{12(\theta - 1)}$, $\varphi_{22} = \frac{\theta}{3} - \frac{\alpha_1 \theta^2 s_*}{3(\theta - 1)}$, $\varphi_{23} = \frac{\alpha_1 \theta^2 s_*}{6(\theta - 1)}$. With $\alpha_1 = -\frac{1}{4}$, we have approximately

$$\mathbb{C} \approx \begin{bmatrix} 2 & 1 & \frac{1}{3} & 0.07226180987 \\ 1 & \frac{2}{3} & -0.01121648833 & -0.004634401251 \\ \frac{1}{3} & -0.01121648833 & 0.1137923368 & 0.01574825186 \\ 0.07226180987 & -0.004634401251 & 0.01574825186 & 0 \end{bmatrix}.$$

One can check that $\rho_c = \rho_d = 2$. Taking $c_0 = 1, c_1 = \frac{1}{10}$ in (3.29), we can get

$$\mathcal{RHS} \leq -\left(\frac{1}{2} - \epsilon\right) \varepsilon_{0}(\|\mathbb{D}_{0}u^{n}\|^{2} + \|\mathbb{D}_{1}u^{n}\|^{2}) - \frac{\tau}{10}(\|\mathbb{D}_{0}q^{n}\|^{2} + \|\mathbb{D}_{1}q^{n}\|^{2}) + \left[2\alpha_{1}\alpha_{2}\theta^{2} - \frac{1}{12} + \varepsilon\right]\|\mathbb{D}_{2}u^{n}\|^{2} + C_{1}(\|\mathbb{D}_{3}u^{n}\|^{2} + \|\mathbb{D}_{4}u^{n}\|^{2}) + \left(C_{2}C_{\nu,\rho}\lambda_{c} + \frac{9C_{\nu,\rho}^{2}}{10}\lambda_{d}\right)(\|\mathbb{D}_{2}u^{n}\|^{2} + \|\mathbb{D}_{3}u^{n}\|^{2}),$$

$$(3.71)$$

for any positive ϵ and ϵ , where $\epsilon_0 = \frac{4-\sqrt{13}}{3}$, C_1 and C_2 are positive constants depending on ϵ and ϵ , respectively. Taking $\epsilon = \frac{1}{2}$ and $\epsilon = \frac{1}{24} - \alpha_1 \alpha_2 \theta^2$, we have

$$\mathcal{RHS} \leq (\alpha_1 \alpha_2 \theta^2 - \frac{1}{24}) \|\mathbb{D}_2 u^n\|^2 - \frac{\tau}{10} (\|\mathbb{D}_0 q^n\|^2 + \|\mathbb{D}_1 q^n\|^2)$$

$$(3.72) + C_1 (\|\mathbb{D}_3 u^n\|^2 + \|\mathbb{D}_4 u^n\|^2) + (C_2 C_{\nu,\rho} \lambda_c + C_{\nu,\rho}^2 \lambda_d) (\|\mathbb{D}_2 u^n\|^2 + \|\mathbb{D}_3 u^n\|^2).$$

Furthermore, the estimates for $\|\mathbb{D}_3 u^n\|$ and $\|\mathbb{D}_4 u^n\|$ are the same as that stated in Lemma 3.4, with different coefficients $s_{\ell i}$ which are listed in Appendix A.6. As a consequence, we can get the same type conclusion regarding numerical stability as for the IMEX(4,4,3)-LDG(k) scheme except with different constants ϱ_1 and ϱ_2 in (3.67).

From the above analysis, we summarize the main conclusions in the following theorem.

Theorem 3.5. The schemes IMEX(1,1,1)-LDG(0), IMEX(2,2,2)-LDG(k) with k=0,1, IMEX(4,4,3)-LDG(k) and IMEX(3,4,3)-LDG(k) with any integer $k\geq 0$ have monotonicity stability under the time step condition

(3.73)
$$\tau \leq \min \left\{ \varrho_1, \varrho_2 P_e \right\} \frac{h}{c} = \min \left\{ \varrho_1, \varrho_2 \frac{h/c}{d/c^2} \right\} \frac{h}{c},$$

where the positive constants ϱ_1 , ϱ_2 are independent of c, d and h, and they depend on each specific IMEX RK method, the polynomial degree k, and the mesh regularity parameter ρ . Particularly, when d=0, we have $P_e=+\infty$ and the time step condition becomes $\tau \leq \varrho_1 h/c$.

Remark 3.6. For the IMEX(1,1,1)-LDG(k) scheme with $k \geq 1$ and the IMEX(2,2,2)-LDG(k) scheme with $k \geq 2$, the exponential-type stability is achieved under more stringent conditions $\tau \lesssim (h/c)^2$ and $\tau \lesssim (h/c)^{4/3}$, respectively, in the convection-dominated regime with $P_e = \frac{h/c}{d/c^2} \gg 1$. The results are consistent to and generalize the stability analysis in [19, 17] when these schemes are applied to the linear convection equation (i.e. (1.1) when d = 0).

4. Stability analysis based on backward temporal differences

The stability results established in [11] indicate that the fully discrete schemes defined in Subsection 2.3 have monotonicity stability if the time step τ satisfies $\tau \lesssim d/c^2$. This result shows that the methods are especially efficient by allowing large time step sizes when d/c^2 is not too small and the problem is relatively in the diffusion-dominated regime. The stability analysis in [11], however, was obtained case by case for each family of the IMEX-LDG(k) method by choosing suitable test functions (also see [6]). In this section, we want to propose a general framework to re-establish the results as in [11], by using a new concept, namely,

backward temporal differences. With some technical details to be the same as those in [11], our presentation will be brief, with the emphasis mainly on the framework. Throughout this section, we assume $d \neq 0$.

We begin with introducing a series of backward temporal differences $\{\mathbb{D}_{\ell}^- w^n\}_{\ell=0}^m$, defined as

(4.1)
$$\mathbb{D}_{\ell}^- w^n = w^{n,m-\ell+1} - w^{n,m-\ell}$$
, $1 \le \ell \le m$, and $\mathbb{D}_0^- w^n = w^{n,m} = w^{n+1}$, for $w = u, q$. Note that

(4.2)
$$w^{n,i} = \mathbb{D}_0^- w^n - \sum_{\kappa=1}^{m-i} \mathbb{D}_{\kappa}^- w^n, \quad \text{for } i = 0, \dots, m.$$

Setting $c_{0i} = d_{0i} = 0$, denoting $a_{\ell i} = c_{m-\ell+1,i} - c_{m-\ell,i}$ and $b_{\ell i} = d_{m-\ell+1,i} - d_{m-\ell,i}$, then from (2.17) and (4.2) we have for $1 \le \ell \le m$ that

$$(\mathbb{D}_{\ell}^{-}u^{n}, v) = \tau \sum_{i=0}^{m_{1}} [a_{\ell i}\mathcal{H}(u^{n,i}, v) + b_{\ell i}\mathcal{L}(q^{n,i}, v)]$$

$$(4.3a) \qquad = \tau \sum_{i=0}^{m_{1}} [a_{\ell i}\mathcal{H}(\mathbb{D}_{0}^{-}u^{n} - \sum_{\kappa=1}^{m-i} \mathbb{D}_{\kappa}^{-}u^{n}, v) + b_{\ell i}\mathcal{L}(\mathbb{D}_{0}^{-}q^{n} - \sum_{\kappa=1}^{m-i} \mathbb{D}_{\kappa}^{-}q^{n}, v)],$$

$$(4.3b) \qquad (\mathbb{D}_{\ell}^{-}q^{n}, r) = \mathcal{K}(\mathbb{D}_{\ell}^{-}u^{n}, r).$$

By taking L^2 -norm on both sides of (4.2) with w = u and i = 0, we get the energy equation

$$(4.4) ||u^{n+1}||^2 - ||u^n||^2 + \mathcal{S} = 2\sum_{\ell=1}^m (\mathbb{D}_{\ell}^- u^n, \mathbb{D}_0^- u^n) - 2\sum_{1 \le j < \ell \le m} (\mathbb{D}_{\ell}^- u^n, \mathbb{D}_j^- u^n),$$

where

(4.5)
$$S = \sum_{\ell=1}^{m} \|\mathbb{D}_{\ell}^{-} u^{n}\|^{2}$$

is the stabilization provided by the time discretization, which plays an important role in this case. Furthermore, the right hand side of (4.4) can be rewritten as the sum of R_c and R_d by using (4.3a), where

(4.6a)

$$R_{c} = 2\tau \left[\sum_{\ell=1}^{m} \sum_{i=0}^{m_{1}} a_{\ell i} \mathcal{H}(\mathbb{D}_{0}^{-} u^{n} - \sum_{\kappa=1}^{m-i} \mathbb{D}_{\kappa}^{-} u^{n}, \mathbb{D}_{0}^{-} u^{n}) - \sum_{1 \leq j < \ell \leq m} \sum_{i=0}^{m_{1}} a_{\ell i} \mathcal{H}(\mathbb{D}_{0}^{-} u^{n} - \sum_{\kappa=1}^{m-i} \mathbb{D}_{\kappa}^{-} u^{n}, \mathbb{D}_{j}^{-} u^{n}) \right],$$
(4.6b)

$$R_d = 2\tau \left[\sum_{\ell=1}^m \sum_{i=0}^{m_1} b_{\ell i} \mathcal{L}(\mathbb{D}_0^- q^n - \sum_{\kappa=1}^{m-i} \mathbb{D}_\kappa^- q^n, \mathbb{D}_0^- u^n) - \sum_{1 \le j < \ell \le m} \sum_{i=0}^{m_1} b_{\ell i} \mathcal{L}(\mathbb{D}_0^- q^n - \sum_{\kappa=1}^{m-i} \mathbb{D}_\kappa^- q^n, \mathbb{D}_j^- u^n) \right],$$

and R_c is related to the convection while R_d is related to the diffusion. Using Corollary 2.4, R_d can be expressed as a quadratic form

$$(4.7) R_d = -\tau \int_{\Omega} \boldsymbol{q}^{n^{\top}} \mathbb{S} \boldsymbol{q}^n dx,$$

with some properly defined q^n and a symmetric matrix \mathbb{S} . Noting that the coefficients $d_{\ell 0} = 0$ in the IMEX schemes presented in Subsection 2.3, so $b_{\ell 0} = 0$, hence

we can define

$$\boldsymbol{q}^n = (\mathbb{D}_0^- q^n, \mathbb{D}_1^- q^n, \cdots, \mathbb{D}_{m-1}^- q^n)^{\top}$$

in general. The definition of q^n is different for the IMEX(3,4,3) scheme, as to be seen in the proof of Theorem 4.3. The matrix \mathbb{S} is determined by the respective IMEX scheme. Depending on the property of \mathbb{S} , our analysis can proceed generally as two cases below, with more details given in the proof of Theorem 4.3 for each family of methods.

Case 1. If the matrix S is positive definite, then

$$R_d \leq -\varepsilon_0 \tau \|\boldsymbol{q}^n\|^2$$
,

where $\|\boldsymbol{q}^n\|^2 = \int_{\Omega} \boldsymbol{q}^{n\top} \boldsymbol{q}^n dx$, and ε_0 denotes the smallest eigenvalue of \mathbb{S} . We define \boldsymbol{u}^n in the same fashion as \boldsymbol{q}^n and define

$$\boldsymbol{u}_{s}^{n}=(\mathbb{D}_{1}^{-}u^{n},\mathbb{D}_{2}^{-}u^{n},\cdots,\mathbb{D}_{m}^{-}u^{n})^{\top}.$$

Note that the entries of \boldsymbol{u}_s^n come from the stabilization term \mathcal{S} , and in general \boldsymbol{u}^n and \boldsymbol{u}_s^n are not the same. One can check that $\sum_{\ell=1}^m \sum_{i=0}^{m_1} a_{\ell i} = 1$, and using this, R_c can be further rewritten as

(4.8)
$$R_c = 2\tau \mathcal{H}(\mathbb{D}_0^- u^n, \mathbb{D}_0^- u^n) + \tau(\boldsymbol{u}^n, \boldsymbol{u}_s^n)_{\mathcal{H}},$$

where

$$(4.9) \qquad (\boldsymbol{u}^n, \boldsymbol{u}_s^n)_{\mathcal{H}} = \sum_{u \in \boldsymbol{u}^n, v \in \boldsymbol{u}_s^n} [c_{uv}^* \mathcal{H}(u, v) + c_{vu}^* \mathcal{H}(v, u)],$$

with some coefficients c_{uv}^* and c_{vu}^* depending on the respective temporal scheme. By writing $u \in \mathbf{u}^n$, we mean u is any entry of \mathbf{u}^n . Now using (2.10a), Lemma 2.3, Lemma 2.6, and Young's inequality, we have

$$R_{c} \leq -c\tau \|\mathbb{D}_{0}^{-}u^{n}\|^{2} + Cc\tau \sum_{u \in \mathbf{u}^{n}, v \in \mathbf{u}_{s}^{n}} \left(\|u_{x}\| + \sqrt{\nu(\rho h)^{-1}} \|u\| \right) \|v\|$$

$$\leq C\bar{C}_{\nu,\rho} \frac{c\tau}{\sqrt{d}} \sum_{q \in \mathbf{q}^{n}, v \in \mathbf{u}_{s}^{n}} \|q\| \|v\|$$

$$\leq \varepsilon_{0}\tau \|\mathbf{q}^{n}\|^{2} + \frac{C^{2}\bar{C}_{\nu,\rho}^{2}}{4\varepsilon_{0}} \frac{c^{2}\tau}{d} \mathcal{S},$$

where C is a positive constant depending on those coefficients c_{uv}^* and c_{vu}^* defined in (4.9), and S is defined in (4.5). Thus we can bound the term R_c using the stability terms $\varepsilon_0 \tau \|\boldsymbol{q}^n\|^2$ and S, by imposing a time step condition $\tau \lesssim d/c^2$.

<u>Case 2.</u> If the matrix \mathbb{S} is not positive definite, then we add $\sum_{\ell=1}^{m-1} c_{\ell} \|\mathbb{D}_{\ell}^{-} u^{n}\|^{2}$ with $c_{\ell} > -1$ to both sides of the energy equation (4.4) and get

(4.10)
$$||u^{n+1}||^2 - ||u^n||^2 + \mathcal{S}' = R_c' + R_d',$$

where
$$S' = S + \sum_{\ell=1}^{m-1} c_{\ell} \|\mathbb{D}_{\ell}^{-} u^{n}\|^{2}$$
 and
$$R'_{c} = R_{c} + \tau \sum_{\ell=1}^{m-1} c_{\ell} \sum_{i=0}^{m_{1}} a_{\ell i} \mathcal{H}(\mathbb{D}_{0}^{-} u^{n} - \sum_{\kappa=1}^{m-i} \mathbb{D}_{\kappa}^{-} u^{n}, \mathbb{D}_{\ell}^{-} u^{n}),$$

$$R'_{d} = R_{d} + \tau \sum_{\ell=1}^{m-1} c_{\ell} \sum_{i=0}^{m_{1}} b_{\ell i} \mathcal{L}(\mathbb{D}_{0}^{-} q^{n} - \sum_{\kappa=1}^{m-i} \mathbb{D}_{\kappa}^{-} q^{n}, \mathbb{D}_{\ell}^{-} u^{n})$$

$$= -\tau \int_{\Omega} q^{n} \mathbb{I} \mathbb{S} q^{n} dx - \tau \sum_{\ell=1}^{m-1} c_{\ell} \sum_{i=0}^{m_{1}} b_{\ell i} (\mathbb{D}_{0}^{-} q^{n} - \sum_{\kappa=1}^{m-i} \mathbb{D}_{\kappa}^{-} q^{n}, \mathbb{D}_{\ell}^{-} q^{n})$$

$$= -\tau \int_{\Omega} q^{n} \mathbb{I} \mathbb{S}' q^{n} dx,$$

due to (4.3a) and Corollary 2.4. Choosing suitable c_{ℓ} (if exists) such that \mathbb{S}' is positive definite, we can then get similar results as Case 1.

Remark 4.1. In the framework outlined above, we establish the energy equation directly by using the relationship between the backward temporal differences. This proof line is different from the previous work such as in [11, 6, 8, 13], where energy equation was established by intuitively choosing suitable test functions.

Remark 4.2. The approach of modifying the matrix \mathbb{S} to a positive definite matrix is not unique, and our adopted approach, namely by adding the term $\sum_{\ell=1}^{m-1} c_{\ell} \|\mathbb{D}_{\ell}^{-} u^{n}\|^{2}$, was also used in [6, 14]. The reason of not adding $\|\mathbb{D}_{m}^{-} u^{n}\|^{2}$ is that $\mathbb{D}_{m}^{-} q^{n}$ is not in the quadratic form (4.7). Indeed, if we add $\|\mathbb{D}_{m}^{-} u^{n}\|^{2}$, this will give arise terms involving $\mathbb{D}_{m}^{-} q^{n}$ that can not be estimated.

We would also like to point out that c_{ℓ} may not always exist. As an example, for the forth order IMEX(5,6,4) scheme proposed in [4], we can not find c_{ℓ} such that the modified matrix is positive definite, hence for this case alternative methods would be needed. Nevertheless, the general framework in this section works well for all the schemes considered in this paper.

Now we present the theorem by the above proof line for the four specific schemes.

Theorem 4.3. All schemes in Subsection 2.3, namely, IMEX(1,1,1)-LDG(k), IMEX(2,2,2)-LDG(k), IMEX(4,4,3)-LDG(k) and IMEX(3,4,3)-LDG(k) with any integer $k \geq 0$ have monotonicity stability under the time step condition $\tau \leq \varrho_3 d/c^2$, where the positive constant ϱ_3 is independent of c, d and h, and it depends on each specific $IMEX\ RK$ method, the polynomial degree k, and the mesh regularity parameter ρ .

Proof. For the IMEX(1,1,1)-LDG(k) scheme, we define $\{\mathbb{D}_{\ell}^{-}u^{n}\}_{\ell=0}^{1}$ and $\{\mathbb{D}_{\ell}^{-}q^{n}\}_{\ell=0}^{1}$. In this case $q^{n}=\mathbb{D}_{0}^{-}q^{n}$ and $\mathbb{S}=[2]$. For the IMEX(2,2,2)-LDG(k) scheme, we define $\{\mathbb{D}_{\ell}^{-}u^{n}\}_{\ell=0}^{2}$ and $\{\mathbb{D}_{\ell}^{-}q^{n}\}_{\ell=0}^{2}$. Now $q^{n}=(\mathbb{D}_{0}^{-}q^{n},\mathbb{D}_{1}^{-}q^{n})^{\top}$ and $\mathbb{S}=\begin{bmatrix}2&-1\\-1&2\gamma\end{bmatrix}$. The matrix \mathbb{S} in each of the first and second order in time schemes is positive definite, therefore we can get the stability results directly.

For the IMEX(4,4,3)-LDG(k) scheme, we define $\{\mathbb{D}_{\ell}^-u^n\}_{\ell=0}^4$ and $\{\mathbb{D}_{\ell}^-q^n\}_{\ell=0}^4$, and then set $\boldsymbol{q}^n=(\mathbb{D}_0^-q^n,\mathbb{D}_1^-q^n,\mathbb{D}_2^-q^n,\mathbb{D}_3^-q^n)^{\top}$. It can be calculated that

(4.11)
$$S = \begin{bmatrix} 2 & -1 & -\frac{2}{3} & -2 \\ -1 & 1 & \frac{2}{3} & 0 \\ -\frac{2}{3} & \frac{2}{3} & \frac{4}{3} & \frac{2}{3} \\ -2 & 0 & \frac{2}{3} & 1 \end{bmatrix},$$

which is not positive definite. So we add $\sum_{\ell=1}^{3} c_{\ell} \|\mathbb{D}_{\ell}^{-} u^{n}\|^{2}$ to both sides of the energy equation, expanding the right hand side leads to $R'_{d} = -\tau \int_{\Omega} \boldsymbol{q}^{n} \, \mathbf{r} \, \mathbf{r}' \, \mathbf{r}$

$$(4.12) S' = S + \begin{bmatrix} 0 & \frac{c_1}{4} & -\frac{c_2}{12} & \frac{c_3}{12} \\ \frac{c_1}{4} & 0 & \frac{c_2}{12} & -c_1 - \frac{c_3}{12} \\ -\frac{c_2}{12} & \frac{c_2}{12} & \frac{2c_2}{3} & \frac{c_3}{3} - \frac{c_3}{12} \\ \frac{c_3}{12} & -c_1 - \frac{c_3}{12} & \frac{c_2}{3} - \frac{c_3}{12} & \frac{c_3}{3} \end{bmatrix}.$$

To make \mathbb{S}' positive definite, we require the leading principal minors are all positive. Particularly we require $c_1 \in (4-4\sqrt{2},4+4\sqrt{2})$ to ensure the 2nd order leading principal minor is positive. Taking $c_1=0$ for simplicity, we further require $c_2 \in (40-24\sqrt{3},40+24\sqrt{3})$ to ensure the 3rd order leading principal minor is positive. Taking $c_2=0$ for simplicity, we further require $c_3 \in (24-8\sqrt{2},24+8\sqrt{2})$ to ensure det $\mathbb{S}'>0$. In fact, with $c_3=22$, the smallest eigenvalue of \mathbb{S}' is about 0.0424. Moreover, R'_c can be also written in the form of (4.8). Hence, we can also get the desired stability result.

For the IMEX(3,4,3)-LDG(k) scheme, we define $\{\mathbb{D}_{\ell}^{-}u^n\}_{\ell=0}^4$ and $\{\mathbb{D}_{\ell}^{-}q^n\}_{\ell=0}^4$. In this case we set $\mathbf{q}^n = (\mathbb{D}_0^{-}q^n - \mathbb{D}_1^{-}q^n, \mathbb{D}_2^{-}q^n, \mathbb{D}_3^{-}q^n)^{\top}$, due to that the last two stages of the implicit part of the IMEX(3,4,3) in (2.21) are the same. Now

(4.13)
$$S = \begin{bmatrix} 2 & -\frac{3-\theta}{2} & -\beta_1 - \theta \\ -\frac{3-\theta}{2} & 1 + \theta & \frac{1+\theta}{2} \\ -\beta_1 - \theta & \frac{1+\theta}{2} & 2\theta \end{bmatrix},$$

which is not positive definite. We then add $c_2 \|\mathbb{D}_2^- u^n\|^2 + c_3 \|\mathbb{D}_3^- u^n\|^2$ to both sides of the energy equation, expanding the right hand side leads to $R'_d = -\tau \int_{\Omega} \boldsymbol{q}^{n^{\top}} \mathbb{S}' \boldsymbol{q}^n dx$, with

$$(4.14) S' = S + \begin{bmatrix} 0 & \frac{c_2}{4}(1-\theta) & \frac{c_3}{4}(1-\theta) \\ \frac{c_2}{4}(1-\theta) & -c_2\frac{1-3\theta}{2} & -\frac{c_2}{2}\beta_1 + \frac{(c_2-c_3)(1-\theta)}{4} \\ \frac{c_3}{4}(1-\theta) & -\frac{c_2}{2}\beta_1 + \frac{(c_2-c_3)(1-\theta)}{4} & -c_3\frac{1-3\theta}{2} \end{bmatrix}.$$

To make \mathbb{S}' positive definite, we require $c_2 \in (-1.74455, 35.39030)$. For simplicity, we take $c_2 = 0$, and with this, we further require $c_3 \in (2.22239, 21.16935)$ to ensure \mathbb{S}' to be positive definite. We now take $c_3 = 4$, and this will result in \mathbb{S}' with its smallest eigenvalue being about 0.11523. Moreover, we can calculate that

$$(4.15) R'_c = 2\tau \mathcal{H}(\mathbb{D}_0^- u^n - \mathbb{D}_1^- u^n, \mathbb{D}_0^- u^n - \mathbb{D}_1^- u^n) + \tau(\boldsymbol{u}^n, \boldsymbol{u}_s^n)_{\mathcal{H}},$$

where $(\boldsymbol{u}^n, \boldsymbol{u}_s^n)_{\mathcal{H}}$ has the same form as that defined in (4.9). Hence, we can also get the desired stability result.

5. Improved result for IMEX(1,1,1)-LDG(0) scheme

Following the two frameworks of analysis in Sections 3-4, some underlying stabilization mechanisms of the IMEX-LDG methods are not fully explored, e.g. the stabilization due to the implicit treatment of the diffusion term within the first framework, or the stabilization associated with the upwind discretization of the convection term within the second framework. Ideally one would want to simultaneously utilize all stabilization mechanisms available to find better time step conditions for stability. Such holistic energy-method based stability analysis however is challenging in general, yet can be carried out for the first order in space and time IMEX(1,1,1)-LDG(0) scheme. This will be shown and discussed next.

We will start with assuming $c, d \neq 0$ and revisiting the analysis for the IMEX(1,1,1)-LDG(0) scheme. In this case, $(q,r)_j = \sqrt{d}[u]_{j-\frac{1}{2}}r^+_{j-\frac{1}{8}}$. Taking r=1, we get

(5.1)
$$\sqrt{d}[u]_{j-\frac{1}{2}} = (q,1)_j \le \sqrt{h_j} ||q||_j.$$

Thus we have

(5.2)
$$\|u\|^2 \le \frac{h}{d} \|q\|^2, \quad \text{or} \quad \|q\|^2 \ge \frac{d}{h} \|u\|^2.$$

From the analysis in Section 4, we have the following energy equation for the IMEX(1,1,1)-LDG(0) scheme

$$(5.3) ||u^{n+1}||^2 - ||u^n||^2 + ||\mathbb{D}_1^- u^n||^2 = -2\tau ||\mathbb{D}_0^- q^n||^2 - c\tau ||\mathbb{D}_0^- u^n||^2 + R,$$

where

(5.4)
$$R = -2\tau \mathcal{H}(\mathbb{D}_1^- u^n, \mathbb{D}_0^- u^n) = -2c\tau \sum_{j=1}^N (\mathbb{D}_1^- u^n)_{j-\frac{1}{2}}^- [\mathbb{D}_0^- u^n]_{j-\frac{1}{2}}.$$

In what follows we present three different ways to derive stability.

• Using the stability terms $\|\mathbb{D}_1^- u^n\|^2$ and $2\tau \|\mathbb{D}_0^- q^n\|^2$. By using the inverse inequality (2.9) and the relationship (5.1) we have

$$(5.5) R \leq 2c\tau \sum_{i=1}^{N} h_{j}^{-1/2} \|\mathbb{D}_{1}^{-}u^{n}\|_{j} \sqrt{\frac{h_{j}}{d}} \|\mathbb{D}_{0}^{-}q^{n}\|_{j} \leq \frac{2c}{\sqrt{d}} \tau \|\mathbb{D}_{1}^{-}u^{n}\| \|\mathbb{D}_{0}^{-}q^{n}\|.$$

Thus we get the monotonicity stability if the quadratic form $\frac{2c}{\sqrt{d}}\tau\|\mathbb{D}_1^-u^n\|\|\mathbb{D}_0^-q^n\|-\|\mathbb{D}_1^-u^n\|^2-2\tau\|\mathbb{D}_0^-q^n\|^2$ stays nonnegative, and this can be ensured by $\frac{c^2\tau^2}{d}\leq 2\tau$, i.e.

(5.6)
$$\tau \le \tau_1 = \frac{2d}{c^2}.$$

• Using the stability terms $\|\mathbb{D}_1^- u^n\|^2$ and $c\tau [\mathbb{D}_0^- u^n]^2$. By using the inverse inequality (2.9) we obtain

(5.7)
$$R \leq 2c\tau \sqrt{(\rho h)^{-1}} \|\mathbb{D}_1^- u^n\| [\mathbb{D}_0^- u^n].$$

Thus, we can get the monotonicity stability if $\frac{c^2\tau^2}{\rho h} \leq c\tau$, i.e.

(5.8)
$$\tau \le \tau_2 = \frac{\rho h}{c}.$$

• Using all the stability terms $\|\mathbb{D}_1^- u^n\|^2$, $\|\mathbb{D}_0^- q^n\|^2$ and $c\tau [\mathbb{D}_0^- u^n]^2$. With the help of (5.2) and (5.7) we have

$$\|u^{n+1}\|^2 - \|u^n\|^2 \le -\|\mathbb{D}_1^- u^n\|^2 - \left(c + \frac{2d}{h}\right)\tau \|\mathbb{D}_0^- u^n\|^2 + 2c\tau \sqrt{(\rho h)^{-1}}\|\mathbb{D}_1^- u^n\| \|\mathbb{D}_0^- u^n\|.$$

Monotonicity stability follows by requiring $c^2\tau^2/(\rho h) \leq (c+2d/h)\tau$, i.e.

(5.10)
$$\tau \le \tau_3 = \rho \left(\frac{h}{c} + \frac{2d}{c^2} \right).$$

One can easily see that (5.6), (5.8), (5.10) also hold when one of the model parameters d and c is zero. From these results, we can reach the following theorem.

Theorem 5.1. The IMEX(1,1,1)-LDG(0) scheme has monotonicity stability under the time step condition

(5.11)
$$\tau \le \max\{\tau_1, \tau_2, \tau_3\} = \max\{\tau_1, \tau_3\} = \max\left(\frac{2d}{c^2}, \rho(\frac{h}{c} + \frac{2d}{c^2})\right).$$

The time step condition (5.11) is an improvement over that in Theorem 2.8 especially in the intermediate regime with moderate $P_e = \frac{h/c}{d/c^2}$, as the analysis in Section 3 alone will lead to $\tau \leq \tau_2$, while the analysis in Section 4 alone will lead to $\tau \leq \tau_1$, therefore the condition in (2.22) will be $\tau \leq \max(\rho h/c, 2d/c^2)$. This observation indicates that the time step condition (2.22) in Theorem 2.8, especially in the intermediate regime, is not sharp.

6. Numerical experiments

In this section, we want to perform some numerical experiments to complement the theoretical analysis. Ideally, we would want to numerically obtain the values of $\varrho_j, j=1,2,3$, in Theorem 2.8, so the condition (2.22) can guide the choice of time step in practice. Yet our improved result for the IMEX(1,1,1)-LDG(0) scheme in Section 5 indicates that the time step condition in (2.22) has not fully captured the time step allowed for monotonicity stability of the methods of our consideration, especially in the intermediate regime. In other words, even though our energy based analysis shows that the time step condition for the monotonicity stability can be expressed as $\tau \leq \mathcal{F}(h/c,d/c^2)$, the result in (2.22) does not seem to provide the right form of the function \mathcal{F} in the intermediate regime in general. It is therefore not wise to numerically fit all the parameters $\varrho_j, j=1,2,3$ in (2.22). Instead in this section, we will present some numerical study to obtain a slightly stricter time step condition in the form of

(6.1)
$$\tau \le \max \left\{ \hat{\varrho}_1 \frac{h}{c}, \hat{\varrho}_3 \frac{d}{c^2} \right\},$$

that ensures monotonicity stability and can be used by practitioners. One can interpret that $\hat{\varrho}_1 = \varrho_1$ or $\hat{\varrho}_1 = \min(\varrho_1, \varrho_2)$, $\hat{\varrho}_3 = \varrho_3$, yet this is not crucial.

To proceed, we will first present Fourier analysis in Section 6.1, which will provide necessary conditions for monotonicity stability when the meshes are uniform, and particularly suggest the time step condition of the form (6.1) with specific values $\hat{\varrho}_1$ and $\hat{\varrho}_3$ for each method. In Section 6.2, we will implement each method through two sets of numerical tests and provide evidence to support the time step condition in (6.1) found in Section 6.1.

6.1. Fourier analysis. To carry out Fourier analysis, we need to assume the mesh is uniform. For a given IMEX(p, r, s)-LDG(k) scheme, we locally expand the numerical solution u^n with respect to the scaled Legendre basis functions, namely

(6.2)
$$u^{n}(x) = \sum_{\ell=0}^{k} u_{j\ell}^{n} \phi_{\ell}^{j}(x), \quad \text{for} \quad x \in I_{j},$$

where $\phi_{\ell}^{j}(x) = \phi_{\ell}(2(x-x_{j})/h)$ and $\{\phi_{\ell}\}_{\ell=0}^{k}$ are the standard Legendre polynomials defined on [-1,1], satisfying $\|\phi_{\ell}(x)\|_{L^{2}[-1,1]} = 1$. Denote $\boldsymbol{u}_{j}^{n} = (u_{j0}^{n}, u_{j1}^{n}, \cdots, u_{jk}^{n})^{\top}$, take the ansatz $\boldsymbol{u}_{j}^{n} = \hat{\boldsymbol{u}}^{n}e^{Ix_{j}n}$, where $I = \sqrt{-1}$ and η is the wave number, then

(6.3)
$$\hat{\boldsymbol{u}}^{n+1} = \boldsymbol{G}(\lambda_{c}, \lambda_{d}; \xi) \hat{\boldsymbol{u}}^{n},$$

where $G(\lambda_c, \lambda_d; \xi)$ is the amplification matrix and $\xi = \eta h$. We will adopt a principle similar to that in [9] to define the stability region: For a pair of λ_c and λ_d , if the eigenvalues $\lambda_i(\xi)$, $i = 0 \cdots k$, of $G(\lambda_c, \lambda_d; \xi)$ satisfy $\max_i \{|\lambda_i(\xi)|\} \leq 1, \forall \xi \in [-\pi, \pi]$, we regard the pair, λ_c and λ_d , fall in the stability region. Such principle is easy to check numerically, yet does not take into account the eigenvectors of G and the algebraic multiplicity of those eigenvalues of modulus 1, hence it only provides a necessary condition for monotonicity stability in general.

A special case is IMEX(1,1,1)-LDG(0) scheme, for which Fourier analysis will result in a 1×1 amplification matrix G, and leads to a sufficient and necessary condition on the time step when the meshes are uniform. In fact this condition can be given analytically as $\tau \leq h/c + 2d/c^2$, and it is identical to what we have obtained by energy based stability in Theorem 5.1, given by (5.11) with $\rho = 1$ for uniform meshes.

For general cases, we will numerically calculate the stability region. With a similar argument as in [9], one can show that $G(\lambda_c, \lambda_d; \xi)$ is similar to some matrix $\hat{G}(\lambda_{\rm c}, \lambda_{\rm c}^2/\lambda_{\rm d}; \xi)$, indicating that the stability region equivalently only depends on $\lambda_{\rm c} = c\tau h^{-1}$ and $\lambda_{\rm c}^2/\lambda_{\rm d} = \tau c^2 d^{-1}$. This is consistent to the results in Theorem 2.8. Next we visualize the stability region in terms of λ_c and λ_c^2/λ_d , following the principle mentioned above. The stability region is computed numerically for each scheme by taking 200 uniform samples of ξ from $[-\pi, \pi]$, with λ_c and λ_c^2/λ_d sampled with a spacing 0.01 over the range [0, 10] and [0, 20], respectively. The results are reported in Figure 1 for the IMEX(1,1,1)-LDG(0) scheme, the IMEX(2,2,2)-LDG(k) scheme with k = 0, 1, the IMEX(4,4,3)-LDG(k) and IMEX(3,4,3)-LDG(k) schemes with k = 1, 2, 3. In all subfigures, the stability regions are always to the left of and below the stability curves. For each scheme, the vertical line within the stability region with the largest x-intercept (see the green line in each subfigure) corresponds to the time step condition $\tau \leq \hat{\varrho}_1 h/c$ in the convection-dominated regime, with the associated x-intercept as $\hat{\varrho}_1$; and the horizontal line within the stability region with the largest y-intercept (see the blue line in each subfigure) corresponds to the time step condition $\tau \leq \hat{\varrho}_3 d/c^2$ in the diffusion-dominated regime, with the associated yintercept as $\hat{\varrho}_3$. The values of $\hat{\varrho}_1$ and $\hat{\varrho}_3$ are numerically extracted for each method and reported in Table 1.

Finally, we conjecture that for each scheme of our consideration, a time step condition as in (6.1) with $\hat{\varrho}_1$ and $\hat{\varrho}_3$ in Table 1 provides a sufficient condition for monotonicity stability. This will be further supported numerically in next subsection.

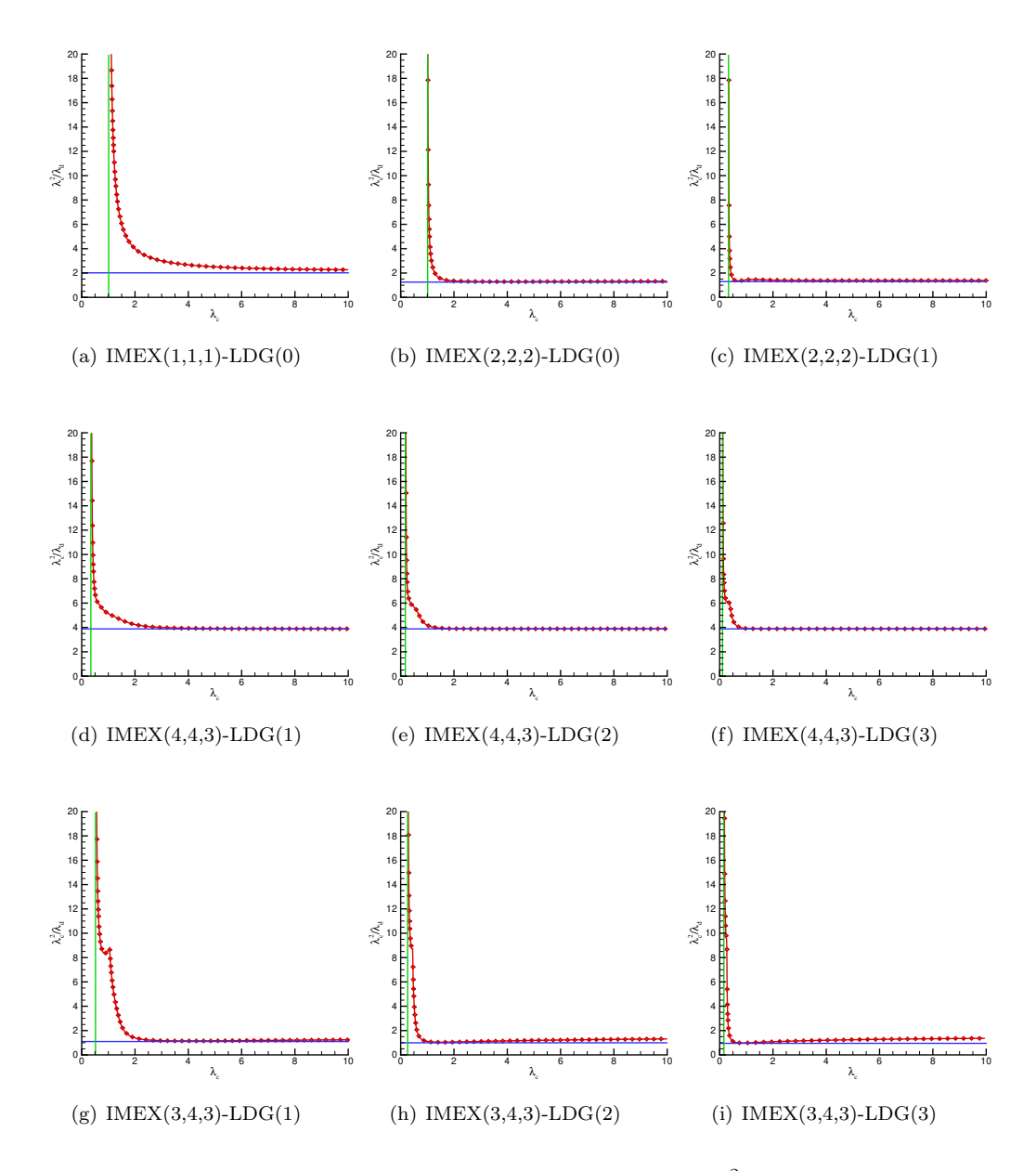


FIGURE 1. Stability curve (red) in terms of λ_c vs. λ_c^2/λ_d , by Fourier analysis with the stability region to the left and below the curve.

6.2. Further numerical validation. In this subsection, we will provide numerical evidence that the time step condition (6.1) with $\hat{\varrho}_1$ and $\hat{\varrho}_3$ in Table 1 can ensure monotonicity stability and provide a sufficient condition. To this end, we consider the model (1.1) with the exact solution $U(x,t) = e^{-dt} \sin(x - ct)$ on the domain $(-\pi, \pi)$. As the first group of tests, we implement the methods on uniform

	\hat{arrho}_1				$\hat{\varrho}_3$			
k	0	1	2	3	0	1	2	3
IMEX(1,1,1)-LDG(k)	1	*	*	*	2	*	*	*
IMEX(2,2,2)-LDG(k)	1	0.333	*	*	1.295	1.350	*	*
IMEX(4,4,3)-LDG(k)	1.071	0.344	0.176	0.109	3.925	3.893	3.893	3.893
IMEX(3,4,3)-LDG(k)	1.525	0.508	0.257	0.159	1.815	1.150	1.045	0.985

TABLE 1. Values of $\hat{\varrho}_1$ and $\hat{\varrho}_3$ in condition (6.1)

meshes with the mesh number N=640, with c=1 and d ranges from 10^{-5} to 10, and thus the Péclet mesh number P_e ranges from 10^3 to 10^{-3} . In Figure 2, we present the time history of the L^2 norm of the numerical solution of u by the schemes of IMEX(1,1,1)-LDG(0), IMEX(2,2,2)-LDG(1), IMEX(4,4,3)-LDG(2) and IMEX(3,4,3)-LDG(2), using the largest time step allowed by (6.1) with $\hat{\varrho}_1$ and $\hat{\varrho}_3$ in Table 1 for each method. One can observe that the L^2 norm of numerical solutions does not increase in time.

As the second group of tests, we numerically compute the maximal value of time step τ_0 to ensure the monotonicity stability for each scheme, and compare it with the formula (6.1) with $\hat{\varrho}_1$ and $\hat{\varrho}_3$ in Table 1. For these tests, we consider the model (1.1) with c=1 and different values of d, the final time is T=100, and the number of uniform mesh elements, N, ranges from 10 to 1440. The value τ_0 in each case for a given method is obtained numerically by a bisection search. That is, we start with an initial interval $(\tau_1, \tau_2) = (0, 1)$. In the first iteration, we set the time step as $\tau = (\tau_1 + \tau_2)/2$ and implement the method. If the L^2 -norm of the numerical solution of u deceases in time, in the sense that $||u^{n+1}|| - ||u^n|| \le 10^{-24}$ (the simulation is carried out in double precision), then we set $\tau_1 = \tau$; otherwise, we set $\tau_2 = \tau$; We repeat the iterations until $|\tau_1 - \tau_2| \le tol$, we then set $\tau_0 = \tau$.

The results are presented in Figures 3-6. Here $tol=10^{-5}$ is used in the stoping criterion. In Figure 3-(a), we present the maximal value of the time step τ_0 numerically computed for the IMEX(1,1,1)-LDG(0), while in Figure 3-(b), the time step is the largest based on the Fourier analysis, namely, $\tau_0 = h/c + d/c^2$. These two sets of results are indistinguishable for the first order IMEX(1,1,1)-LDG(0) scheme. Figures 4-6 are for the schemes IMEX(2,2,2)-LDG(1), IMEX(4,4,3)-LDG(2), and IMEX(3,4,3)-LDG(2), respectively. In each figure, the result in subfigure (a) is obtained numerically, and the result in subfigure (b) is determined by the condition (6.1) with $\hat{\varrho}_1$ and $\hat{\varrho}_3$ given in Table 1. The main observation is that the numerically obtained τ_0 is no smaller than that predicted by (6.1), evidencing that (6.1) provides a sufficient condition for the monotonicity stability.

7. Conclusions

Convection-diffusion equations provide mathematical description for many physical applications involving both convection and diffusion effects. Depending on the applications, the model can be relatively diffusion-dominated or convection-dominated, and it can also be convection-dominated only in some sub-regions. When designing numerical methods, it is important that they can work well uniformly with both effects. In this paper, we perform numerical analysis and establish

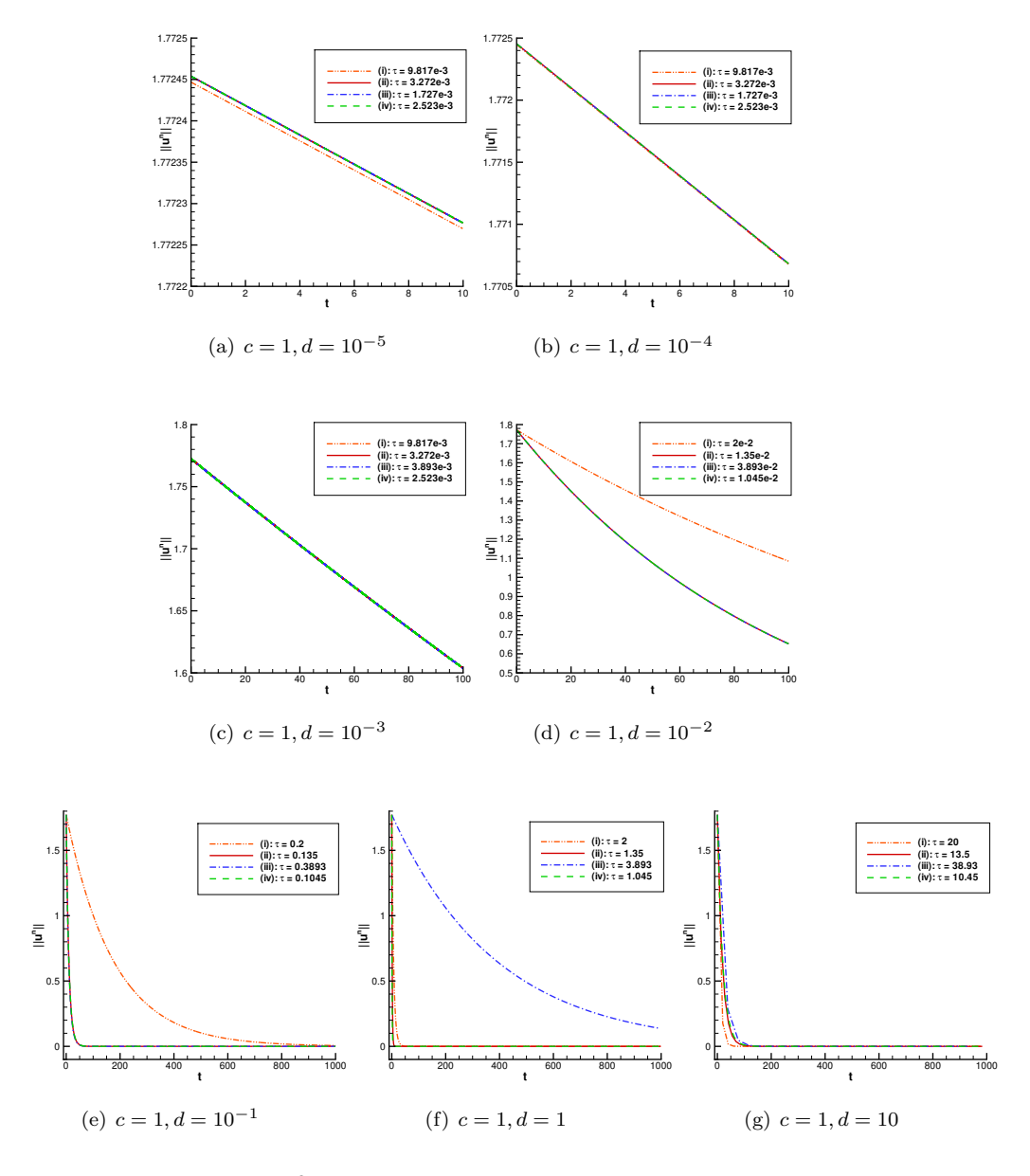


FIGURE 2. The L^2 norm of numerical solution u for each scheme, where (I)-(IV) correspond to the schemes $\mathrm{IMEX}(1,1,1)$ - $\mathrm{LDG}(0)$, $\mathrm{IMEX}(2,2,2)$ - $\mathrm{LDG}(1)$, $\mathrm{IMEX}(4,4,3)$ - $\mathrm{LDG}(2)$ and $\mathrm{IMEX}(3,4,3)$ - $\mathrm{LDG}(2)$, respectively.

uniform stability for several IMEX-LDG methods solving the linear convectiondiffusion equation in one dimension with periodic boundary conditions. Particularly, following the energy-method based analysis in two general frameworks, we show that the schemes being considered have monotonicity stability under the time

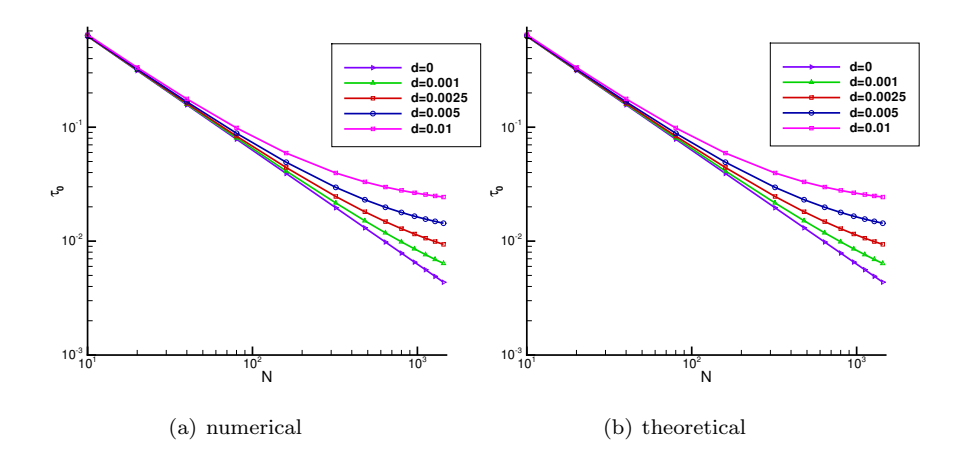


FIGURE 3. The maximal value of time step to ensure monotonicity stability for scheme IMEX(1,1,1)-LDG(0). (a) numerical; (b) theoretically obtained in Theorem 5.1 and also by Fourier analysis.

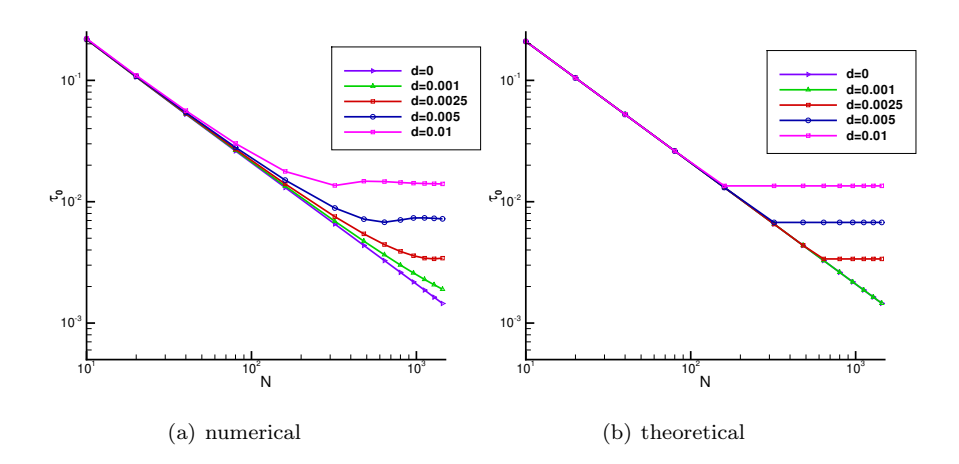


FIGURE 4. The maximal value of time step to ensure monotonicity stability for scheme IMEX(2,2,2)-LDG(1). (a) numerical; (b) theoretical by Fourier analysis.

step conditions $\tau = \mathcal{F}(h/c, d/c^2)$, which become known time step conditions in the diffusion-dominated and convection-dominated regimes, respectively. By exploring all stabilization mechanisms available, an improved time step condition is obtained for the first order IMEX(1,1,1)-LDG(0) scheme. Similar holistic energy-based stability analysis seems to be challenging for the IMEX-LDG methods of higher than first order temporal accuracy, and this will be left for our future exploration. We would also like to investigate uniform stability for numerical methods solving other PDE models, e.g. the Navier–Stokes equations.

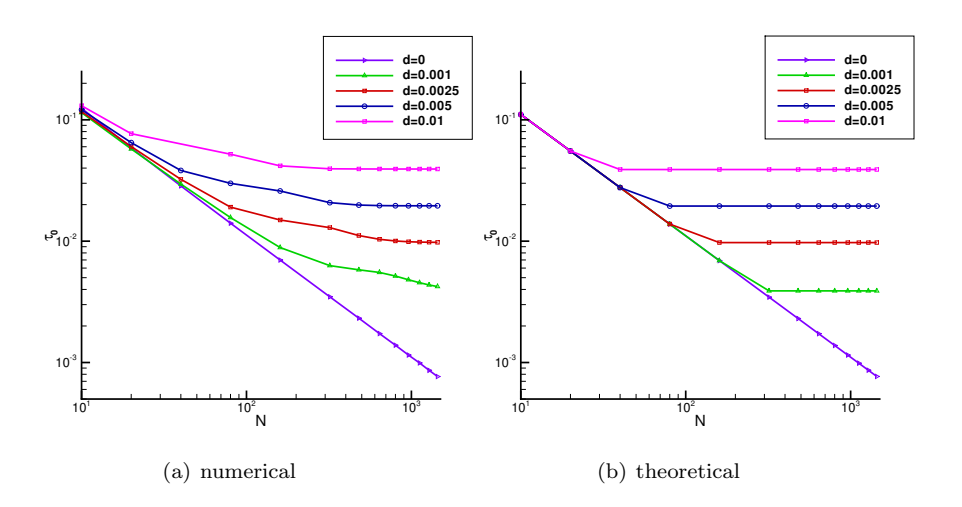


FIGURE 5. The maximal value of time step to ensure monotonicity stability for scheme IMEX(4,4,3)-LDG(2). (a) numerical; (b) theoretical by Fourier analysis.

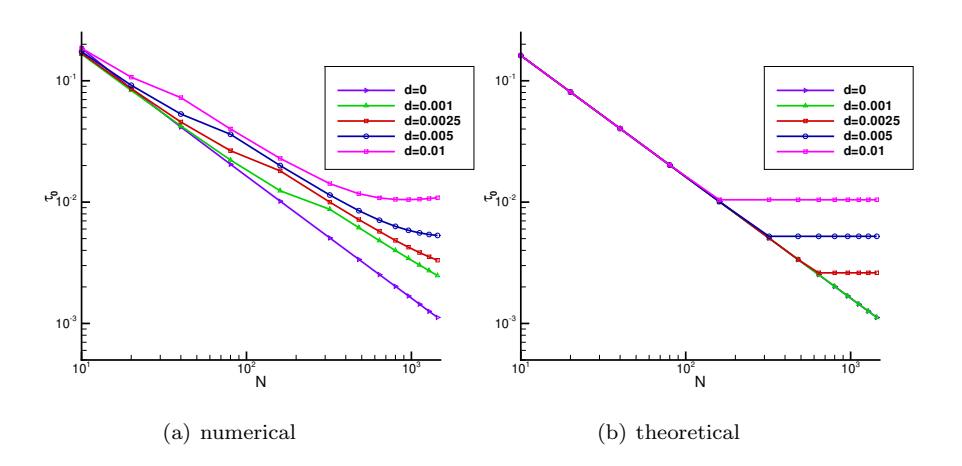


FIGURE 6. The maximal value of time step to ensure monotonicity stability for scheme $\mathrm{IMEX}(3,4,3)\text{-}\mathrm{LDG}(2)$. (a) numerical; (b) theoretical by Fourier analysis.

APPENDIX

A.1: The detail derivation of Algorithms 1 and 2. Multiplying $\sigma_{\kappa\ell}$ on both sides of (2.17a) and adding up from $\ell = 1$ to $\ell = \kappa$, we can get

(A.1)
$$(\sum_{1\leq\ell\leq\kappa}\sigma_{\kappa\ell}u^{n,\ell} - \sum_{1\leq\ell\leq\kappa}\sigma_{\kappa\ell}u^{n}, v) = \tau\mathcal{H}(\sum_{1\leq\ell\leq\kappa}\sigma_{\kappa\ell}\sum_{0\leq i\leq\ell-1}c_{\ell i}u^{n,i}, v) + \tau\mathcal{L}(\sum_{1\leq\ell\leq\kappa}\sigma_{\kappa\ell}\sum_{0\leq i\leq\ell}d_{\ell i}q^{n,i}, v),$$

since $c_{\ell i} = 0$ for $i \ge \ell$ and $d_{\ell i} = 0$ for $i > \ell$. So letting $\sigma_{\kappa 0} = -\sum_{1 \le \ell \le \kappa} \sigma_{\kappa \ell}$, we have

$$(A.2) \qquad (\mathbb{D}_{\kappa}u^{n}, v) = \tau \mathcal{H}(\sum_{1 \leq \ell \leq \kappa} \sigma_{\kappa\ell} \sum_{0 \leq i \leq \ell-1} c_{\ell i}u^{n,i}, v) + \tau \mathcal{L}(\sum_{1 \leq \ell \leq \kappa} \sigma_{\kappa\ell} \sum_{0 \leq i \leq \ell} d_{\ell i}q^{n,i}, v).$$

On the other hand, by the relationship (3.3), we have

$$(A.3) \qquad (\mathbb{D}_{\kappa}u^{n}, v) = \tau \mathcal{H}(\sum_{0 \leq i \leq \kappa - 1} \sigma_{\kappa - 1, i}u^{n, i}, v) + \tau \mathcal{L}(\sum_{0 \leq \ell \leq m_{1}} s_{\kappa \ell} \sum_{0 \leq i \leq \ell} \sigma_{\ell i}q^{n, i}, v).$$

By matching the first term on the right hand sides of (A.2) and (A.3), we get

(A.4)
$$\sum_{1 < \ell < \kappa} \sigma_{\kappa \ell} c_{\ell i} = \sigma_{\kappa - 1, i}, \quad \text{for} \quad 0 \le i \le \kappa - 1,$$

which leads to Algorithm 1.

In addition, given that $s_{\kappa\ell}=0$ when $\ell>\hat{m}_{\kappa}=\min\{m_1,\kappa\}$, and $\sigma_{\ell i}=d_{\ell i}=0$ for $i>\ell$, we know that the second term on the right hand side of (A.2) and (A.3) can be written as $\tau\mathcal{L}(\sum_{1\leq\ell\leq\kappa}\sigma_{\kappa\ell}\sum_{0\leq i\leq\hat{m}_{\kappa}}d_{\ell i}q^{n,i},v)$ and $\tau\mathcal{L}(\sum_{0\leq\ell\leq\hat{m}_{\kappa}}s_{\kappa\ell}\sum_{0\leq i\leq\hat{m}_{\kappa}}\sigma_{\ell i}q^{n,i},v)$, respectively, thus by matching these two terms, we get

(A.5)
$$\sum_{0 \le \ell \le \hat{m}_{\kappa}} s_{\kappa \ell} \sigma_{\ell i} = \sum_{1 \le \ell \le \kappa} \sigma_{\kappa \ell} d_{\ell i}, \quad \text{for} \quad 0 \le i \le \hat{m}_{\kappa},$$

which leads to Algorithm 2.

A.2: The proof for Lemma 3.1. Case 1: for $k \ge 1$. Taking $v = \mathbb{D}_1 u^n$ in (3.3) with $\kappa = 1$, we get

$$\|\mathbb{D}_{1}u^{n}\|^{2} = \tau \mathcal{H}(\mathbb{D}_{0}u^{n}, \mathbb{D}_{1}u^{n}) + \tau \mathcal{L}(\mathbb{D}_{0}q^{n}, \mathbb{D}_{1}u^{n}) + \tau \mathcal{L}(\mathbb{D}_{1}q^{n}, \mathbb{D}_{1}u^{n})$$

$$\leq C_{\nu,\rho}\lambda_{c}\|\mathbb{D}_{0}u^{n}\|\|\mathbb{D}_{1}u^{n}\| - \tau(\mathbb{D}_{0}q^{n}, \mathbb{D}_{1}q^{n}) - \tau\|\mathbb{D}_{1}q^{n}\|^{2}$$

$$\leq \frac{1}{2}\|\mathbb{D}_{1}u^{n}\|^{2} + \frac{C_{\nu,\rho}^{2}\lambda_{c}^{2}}{2}\|\mathbb{D}_{0}u^{n}\|^{2} + \frac{\tau}{4}\|\mathbb{D}_{0}q^{n}\|^{2},$$
(A.6)

where (2.11c) and Corollary 2.4 are used in the second step and the Young's inequality is used in the last step. Then we can get (3.33) directly.

Case 2: for k = 0. Similarly as above, we have

$$\|\mathbb{D}_{1}u^{n}\|^{2} = -c\tau \sum_{j} [\mathbb{D}_{0}u^{n}]_{j-\frac{1}{2}} (\mathbb{D}_{1}u^{n})_{j-\frac{1}{2}}^{+} - \tau(\mathbb{D}_{0}q^{n}, \mathbb{D}_{1}q^{n}) - \tau \|\mathbb{D}_{1}q^{n}\|^{2}$$

$$(A.7) \qquad \leq \frac{1}{2} \|\mathbb{D}_{1}u^{n}\|^{2} + \frac{C_{\nu,\rho}\lambda_{c}}{2} c\tau \|\mathbb{D}_{0}u^{n}\|^{2} + \frac{\tau}{4} \|\mathbb{D}_{0}q^{n}\|^{2},$$

where the inverse inequality (2.9) and the Young's inequality are used in the last step. Thus we can get (3.34).

A.3: The proof for Lemma 3.2. Case 1: for $k \ge 2$. Taking $v = \mathbb{D}_2 u^n$ in (3.3) with $\kappa = 2$ and $\{s_{\kappa\ell}\}$ in (3.42), and following a similar argument as for (A.6), we

can get

$$\|\mathbb{D}_{2}u^{n}\|^{2} = \tau \mathcal{H}(\mathbb{D}_{1}u^{n}, \mathbb{D}_{2}u^{n}) + 2\gamma(1 - \gamma)\tau \mathcal{L}(\mathbb{D}_{1}q^{n}, \mathbb{D}_{2}u^{n}) + \gamma\tau \mathcal{L}(\mathbb{D}_{2}q^{n}, \mathbb{D}_{2}u^{n})$$

$$\leq C_{\nu,\rho}\lambda_{c}\|\mathbb{D}_{1}u^{n}\|\|\mathbb{D}_{2}u^{n}\| - 2\gamma(1 - \gamma)\tau(\mathbb{D}_{1}q^{n}, \mathbb{D}_{2}q^{n}) - \gamma\tau\|\mathbb{D}_{2}q^{n}\|^{2}$$

$$\leq \frac{1}{2}\|\mathbb{D}_{2}u^{n}\|^{2} + \frac{C_{\nu,\rho}^{2}\lambda_{c}^{2}}{2}\|\mathbb{D}_{1}u^{n}\|^{2} + \gamma(1 - \gamma)^{2}\tau\|\mathbb{D}_{1}q^{n}\|^{2}.$$
(A.8)

As a result,

(A.9)

$$\|\mathbb{D}_2 u^n\|^2 \le C_{\nu,\rho}^2 \lambda_c^2 \|\mathbb{D}_1 u^n\|^2 + 2\gamma (1-\gamma)^2 \tau \|\mathbb{D}_1 q^n\|^2 = C_{\nu,\rho}^2 \lambda_c^2 \|\mathbb{D}_1 u^n\|^2 + \gamma \tau \|\mathbb{D}_1 q^n\|^2,$$

since $2\gamma(1-\gamma)^2 = \gamma$.

Similarly, taking $v = \mathbb{D}_1 u^n$ in (3.3) with $\kappa = 1$ and $\{s_{\kappa\ell}\}$ in (3.42), we get

$$\|\mathbb{D}_{1}u^{n}\|^{2} = \tau \mathcal{H}(\mathbb{D}_{0}u^{n}, \mathbb{D}_{1}u^{n}) + \gamma \tau \mathcal{L}(\mathbb{D}_{1}q^{n}, \mathbb{D}_{1}u^{n}) + \tau \mathcal{L}(\mathbb{D}_{0}q^{n}, \mathbb{D}_{1}u^{n})$$

$$\leq C_{\nu,\rho}\lambda_{c}\|\mathbb{D}_{0}u^{n}\|\|\mathbb{D}_{1}u^{n}\| - \gamma \tau \|\mathbb{D}_{1}q^{n}\|^{2} - \tau(\mathbb{D}_{1}q^{n}, \mathbb{D}_{0}q^{n})$$

(A.10)
$$\leq \frac{1}{2} \|\mathbb{D}_1 u^n\|^2 + \frac{C_{\nu,\rho}^2 \lambda_c^2}{2} \|\mathbb{D}_0 u^n\|^2 + \frac{\tau}{4\gamma} \|\mathbb{D}_0 q^n\|^2,$$

Thus,

(A.11)
$$\|\mathbb{D}_1 u^n\|^2 \le C_{\nu,\rho}^2 \lambda_c^2 \|\mathbb{D}_0 u^n\|^2 + \frac{\tau}{2\gamma} \|\mathbb{D}_0 q^n\|^2.$$

Substituting (A.11) into (A.9), we get (3.47).

<u>Case 2: for $k \leq 1$.</u> Following the technique used in [19], we define $w^n = \mathbb{D}_1 u^n - \overline{\mathbb{D}_1 u^n}$, where $\overline{\mathbb{D}_1 u^n}|_{I_j} = \frac{1}{h_j} \int_{I_j} \mathbb{D}_1 u^n dx$. Then we have $(w^n, v_0) = 0$, for any piecewise constant v_0 . So

(A.12)
$$||w^n||^2 = (w^n, w^n) = (\mathbb{D}_1 u^n - \overline{\mathbb{D}_1 u^n}, w^n) = (\mathbb{D}_1 u^n, w^n).$$

Taking $v = w^n$ in (3.3) with $\kappa = 1$, we get

$$||w^n||^2 = \tau \mathcal{H}(\mathbb{D}_0 u^n, w^n) + \gamma \tau \mathcal{L}(\mathbb{D}_1 q^n, w^n) + \tau \mathcal{L}(\mathbb{D}_0 q^n, w^n)$$

$$= -c\tau \sum_{i=1}^{N} \left(((\mathbb{D}_{0}u^{n})_{x}, w^{n})_{j} + [\mathbb{D}_{0}u^{n}]_{j-\frac{1}{2}}(w^{n})_{j-\frac{1}{2}}^{+} \right) + \gamma\tau \mathcal{L}(\mathbb{D}_{1}q^{n}, w^{n}) + \tau \mathcal{L}(\mathbb{D}_{0}q^{n}, w^{n})$$

(A.13)

$$= -c\tau \sum_{j=1}^{N} [\mathbb{D}_{0}u^{n}]_{j-\frac{1}{2}}(w^{n})_{j-\frac{1}{2}}^{+} + \gamma\tau \mathcal{L}(\mathbb{D}_{1}q^{n}, w^{n}) + \tau \mathcal{L}(\mathbb{D}_{0}q^{n}, w^{n}).$$

By the inverse inequality (2.9) and (2.11c), we have

$$(A.14) ||w^n||^2 \le \tau [c\sqrt{\nu(\rho h)^{-1}} [\![\mathbb{D}_0 u^n]\!] + \sqrt{d} C_{\nu,\rho} h^{-1} (\gamma |\![\mathbb{D}_1 q^n |\!] + |\![\mathbb{D}_0 q^n |\!])] |\![w^n |\!].$$

Hence

(A.15)
$$||w^n|| \le \tau [c\sqrt{\nu(\rho h)^{-1}} [|\mathbb{D}_0 u^n|] + \sqrt{d} C_{\nu,\rho} h^{-1} (\gamma ||\mathbb{D}_1 q^n|| + ||\mathbb{D}_0 q^n||)].$$

In addition, by the inverse inequality (2.8), we have

$$\|(\mathbb{D}_1 u^n)_x\| = \|(w^n)_x\| \le \nu(\rho h)^{-1} \|w^n\|$$

$$(A.16) \leq \tau \nu(\rho h)^{-1} [c\sqrt{\nu(\rho h)^{-1}} [\mathbb{D}_0 u^n] + \sqrt{d} C_{\nu,\rho} h^{-1} (\gamma ||\mathbb{D}_1 q^n|| + ||\mathbb{D}_0 q^n||)].$$

Then a slight modification with (A.8) leads to

$$\begin{split} \|\mathbb{D}_{2}u^{n}\|^{2} &= \tau \mathcal{H}(\mathbb{D}_{1}u^{n}, \mathbb{D}_{2}u^{n}) + 2\gamma(1 - \gamma)\tau \mathcal{L}(\mathbb{D}_{1}q^{n}, \mathbb{D}_{2}u^{n}) + \gamma\tau \mathcal{L}(\mathbb{D}_{2}q^{n}, \mathbb{D}_{2}u^{n}) \\ &\leq c\tau(\|(\mathbb{D}_{1}u^{n})_{x}\| + \sqrt{\nu(\rho h)^{-1}} [\![\mathbb{D}_{1}u^{n}]\!]) \|\mathbb{D}_{2}u^{n}\| + \gamma(1 - \gamma)^{2}\tau \|\mathbb{D}_{1}q^{n}\|^{2} \\ &\leq \sqrt{c\tau} [(C_{\nu,\rho}\lambda_{c})^{\frac{3}{2}} [\![\mathbb{D}_{0}u^{n}]\!] + (C_{\nu,\rho}\lambda_{c})^{\frac{1}{2}} [\![\mathbb{D}_{1}u^{n}]\!]] \|\mathbb{D}_{2}u^{n}\| \\ &+ C_{\nu,\rho}^{2}\lambda_{c}\lambda_{d}^{\frac{1}{2}}\sqrt{\tau}(\gamma\|\mathbb{D}_{1}q^{n}\| + \|\mathbb{D}_{0}q^{n}\|) \|\mathbb{D}_{2}u^{n}\| + \gamma(1 - \gamma)^{2}\tau\|\mathbb{D}_{1}q^{n}\|^{2} \\ &\leq \frac{1}{2} \|\mathbb{D}_{2}u^{n}\|^{2} + 2c\tau[(C_{\nu,\rho}\lambda_{c})^{3} [\![\mathbb{D}_{0}u^{n}]\!]^{2} + C_{\nu,\rho}\lambda_{c} [\![\mathbb{D}_{1}u^{n}]\!]^{2}] \\ &+ 2C_{\nu,\rho}^{4}\lambda_{c}^{2}\lambda_{d}\tau(\gamma\|\mathbb{D}_{1}q^{n}\|^{2} + \|\mathbb{D}_{0}q^{n}\|^{2}) + \gamma(1 - \gamma)^{2}\tau\|\mathbb{D}_{1}q^{n}\|^{2}. \end{split}$$

Hence we can arrive at (3.48) in the case $k \leq 1$.

A.4: The proof for Lemma 3.4. Taking $v = \mathbb{D}_3 u^n$ in (3.3) with $\kappa = 3$ and $\{s_{\kappa\ell}\}$ in (3.58), we get

$$\|\mathbb{D}_{3}u^{n}\|^{2} = \tau \mathcal{H}(\mathbb{D}_{2}u^{n}, \mathbb{D}_{3}u^{n}) + \tau \sum_{\ell=1}^{3} s_{3\ell} \mathcal{L}(\mathbb{D}_{\ell}q^{n}, \mathbb{D}_{3}u^{n})$$

$$\leq C_{\nu,\rho}\lambda_{c}\|\mathbb{D}_{2}u^{n}\|\|\mathbb{D}_{3}u^{n}\| + \sqrt{d}C_{\nu,\rho}\tau h^{-1} \sum_{\ell=1}^{2} |s_{3\ell}|\|\mathbb{D}_{\ell}q^{n}\|\|\mathbb{D}_{3}u^{n}\| - \frac{1}{2}\tau\|\mathbb{D}_{3}q^{n}\|^{2}$$

$$\leq \frac{1}{2}\|\mathbb{D}_{3}u^{n}\|^{2} + C_{\nu,\rho}^{2}\lambda_{c}^{2}\|\mathbb{D}_{2}u^{n}\|^{2} + 2C_{\nu,\rho}^{2}\lambda_{d}\tau \sum_{\ell=1}^{2} s_{3\ell}^{2}\|\mathbb{D}_{\ell}q^{n}\|^{2}$$

$$\leq \frac{1}{2}\|\mathbb{D}_{3}u^{n}\|^{2} + C_{\nu,\rho}^{2}\lambda_{c}^{2}\|\mathbb{D}_{2}u^{n}\|^{2} + 2s_{31}^{2}C_{\nu,\rho}^{2}\lambda_{d}\tau\|\mathbb{D}_{1}q^{n}\|^{2} + 2s_{32}^{2}C_{\nu,\rho}^{4}\lambda_{d}^{2}\|\mathbb{D}_{2}u^{n}\|^{2}$$

$$\leq \frac{1}{2}\|\mathbb{D}_{3}u^{n}\|^{2} + C_{\nu,\rho}^{2}\lambda_{c}^{2}\|\mathbb{D}_{2}u^{n}\|^{2} + 2s_{31}^{2}C_{\nu,\rho}^{2}\lambda_{d}\tau\|\mathbb{D}_{1}q^{n}\|^{2} + 2s_{32}^{2}C_{\nu,\rho}^{4}\lambda_{d}^{2}\|\mathbb{D}_{2}u^{n}\|^{2}$$

where (2.11c) and (2.13) are used in the second step, the Young's inequality and Corollary 2.5 are used in the third and the last step, respectively. As a result, we have

$$(A.19) \|\mathbb{D}_3 u^n\|^2 \le (2C_{\nu,\rho}^2 \lambda_{\mathbf{c}}^2 + 4s_{32}^2 C_{\nu,\rho}^4 \lambda_{\mathbf{d}}^2) \|\mathbb{D}_2 u^n\|^2 + 4s_{31}^2 C_{\nu,\rho}^2 \lambda_{\mathbf{d}} \tau \|\mathbb{D}_1 q^n\|^2.$$

Similarly, we can get

$$(A.20) \\ \| \mathbb{D}_4 u^n \|^2 \leq (2C_{\nu,\rho}^2 \lambda_{\mathrm{c}}^2 + 6s_{43}^2 C_{\nu,\rho}^4 \lambda_{\mathrm{d}}^2) \| \mathbb{D}_3 u^n \|^2 + 6s_{42}^2 C_{\nu,\rho}^4 \lambda_{\mathrm{d}}^2 \| \mathbb{D}_2 u^n \|^2 + 6s_{41}^2 C_{\nu,\rho}^2 \lambda_{\mathrm{d}} \tau \| \mathbb{D}_1 q^n \|^2.$$

Substituting (A.19) into (A.20) we get (3.64).

A.5: The coefficients of $\{\sigma_{\kappa\ell}\}$ in (3.2) for IMEX(3,4,3)-LDG(k) scheme.

$$\begin{split} &\sigma_{11} = \frac{1}{\theta}, \quad \sigma_{21} = -\frac{1+\theta}{2\alpha_{1}\theta^{2}}, \quad \sigma_{22} = \frac{1}{\alpha_{1}\theta} \\ &\sigma_{31} = -\frac{\alpha_{2}\theta^{2} + 4\alpha_{1}\theta - 2\theta^{2} - \alpha_{2} - 2\theta}{4\alpha_{1}^{2}\alpha_{2}\theta^{3}}, \quad \sigma_{32} = \frac{\alpha_{2}\theta - \alpha_{2} - 2\theta}{2\alpha_{1}^{2}\alpha_{2}\theta^{2}}, \quad \sigma_{33} = \frac{1}{\alpha_{1}\alpha_{2}\theta} \\ &\sigma_{41} = -\frac{1}{8\alpha_{1}^{3}\alpha_{2}^{2}\theta^{4}} (4\alpha_{1}\alpha_{2}\theta^{3} + \alpha_{2}^{2}\theta^{3} + 8\alpha_{1}^{2}\alpha_{2}\theta - 8\alpha_{1}^{2}\beta_{2}\theta + 4\alpha_{1}\beta_{2}\theta^{2} - \alpha_{2}^{2}\theta^{2} - 4\alpha_{2}\theta^{3} \\ &- 12\alpha_{1}\alpha_{2}\theta + 4\alpha_{1}\beta_{2}\theta - 8\alpha_{1}\theta^{2} - \alpha_{2}^{2}\theta + 4\theta^{3} + \alpha_{2}^{2} + 4\alpha_{2}\theta + 4\theta^{2}), \\ &\sigma_{42} = \frac{4\alpha_{1}\alpha_{2}\theta^{2} + \alpha_{2}^{2}\theta^{2} - 8\alpha_{1}\alpha_{2}\theta + 4\alpha_{1}\beta_{2}\theta - 2\alpha_{2}^{2}\theta - 4\alpha_{2}\theta^{2} + \alpha_{2}^{2} + 4\alpha_{2}\theta + 4\theta^{2}}{4\alpha_{1}^{3}\alpha_{2}^{2}\theta^{3}}, \\ &\sigma_{43} = -\frac{2\alpha_{1}\beta_{2} - \alpha_{2}\theta + \alpha_{2} + 2\theta}{2\alpha_{1}^{2}\alpha_{2}^{2}\theta^{2}}, \quad \sigma_{44} = \frac{1}{\alpha_{1}\alpha_{2}\theta^{2}}, \\ &\sigma_{00} = 1, \quad \sigma_{\kappa 0} = -\sum_{1 \leq \ell \leq \kappa} \sigma_{\kappa \ell}, \ \kappa = 1 \cdots 4. \end{split}$$

Noted that we have used the relation $\beta_1 = 1 - \theta - \beta_2$ to simplify $\sigma_{40}, \dots, \sigma_{44}$.

A.6: The coefficients of $\{s_{\kappa\ell}\}$ in (3.3) for IMEX(3,4,3)-LDG(k) scheme.

$$\begin{split} s_{10} &= 1, \quad s_{11} = \theta \\ s_{20} &= 0, \quad s_{21} = \frac{1-\theta}{2\alpha_{1}}, \quad s_{22} = \theta \\ s_{30} &= 0, \quad s_{31} = -\frac{2\alpha_{1}\beta_{2}\theta + 4\alpha_{1}\theta^{2} + \alpha_{2}\theta^{2} - 2\alpha_{1}\beta_{2} - 4\alpha_{1}\theta - 2\alpha_{2}\theta - 2\theta^{2} + \alpha_{2} + 2\theta}{4\alpha_{1}^{2}\alpha_{2}\theta} \\ s_{32} &= \frac{\beta_{2}}{\alpha_{2}}, \quad s_{33} = \theta \\ s_{40} &= 0, \\ s_{41} &= -\frac{1}{8\alpha_{1}^{3}\alpha_{2}^{2}\theta^{2}} (4\alpha_{1}^{2}\alpha_{2}\beta_{2}\theta + 8\alpha_{1}^{2}\alpha_{2}\theta^{2} - 4\alpha_{1}^{2}\beta_{2}^{2}\theta - 8\alpha_{1}^{2}\beta_{2}\theta^{2} + 2\alpha_{1}\alpha_{2}\beta_{2}\theta^{2} \\ &\quad + 8\alpha_{1}\alpha_{2}\theta^{3} + \alpha_{2}^{2}\theta^{3} - 4\alpha_{1}^{2}\alpha_{2}\beta_{2} - 8\alpha_{1}^{2}\alpha_{2}\theta + 4\alpha_{1}^{2}\beta_{2}^{2} + 8\alpha_{1}^{2}\beta_{2}\theta - 4\alpha_{1}\alpha_{2}\beta_{2}\theta \\ &\quad - 20\alpha_{1}\alpha_{2}\theta^{2} - 8\alpha_{1}\theta^{3} - 3\alpha_{2}^{2}\theta^{2} - 4\alpha_{2}\theta^{3} + 2\alpha_{1}\alpha_{2}\beta_{2} + 12\alpha_{1}\alpha_{2}\theta \\ &\quad + 8\alpha_{1}\theta^{2} + 3\alpha_{2}^{2}\theta + 8\alpha_{2}\theta^{2} + 4\theta^{3} - \alpha_{2}^{2} - 4\alpha_{2}\theta - 4\theta^{2}) \\ s_{42} &= \frac{2\alpha_{1}\alpha_{2}\beta_{2} - 2\alpha_{1}\beta_{2}^{2} - \alpha_{2}^{2}\theta + 2\alpha_{2}\beta_{2}\theta + 2\alpha_{2}\theta^{2} + \alpha_{2}^{2} - 2\alpha_{2}\beta_{2} - 2\alpha_{2}\theta - 2\beta_{2}\theta}{2\alpha_{1}\alpha_{2}^{2}\theta} \\ s_{43} &= \frac{2\alpha_{1}\alpha_{2} - 2\alpha_{1}\beta_{2} + \alpha_{2}\theta - \alpha_{2} - 2\theta}{2\alpha_{1}\alpha_{2}} \end{split}$$

References

- 1. R. A. Adams, Sobolev Spaces, New York, Academic Press, 1975.
- U. M. ASCHER, S. J. RUUTH AND R. J. SPITERI, Implicit-explicit Runge-Kutta methods for time-dependent partial differential equations, Appl. Numer. Math., 25 (1997), pp. 151–167.
- S. BOSCARINO, L. PARESCHI, AND G. RUSSO, Implicit-explicit Runge-Kutta schemes for hyperbolic systems and kinetic equations in the diffusion limit, SIAM J. Sci. Comput., 35 (2013), pp. A22-A51.
- M. P. Calvo, J. De Frutos and J. Novo, Linearly implicit Runge-Kutta methods for advection-reaction-diffusion equations, Appl. Numer. Math., 37 (2001), pp. 535–549.

- B. COCKBURN AND C. -W. SHU, The local discontinuous Galerkin method for time-dependent convection-diffusion systems, SIAM J. Numer. Anal., 35 (1998), pp. 2440–2463.
- G. Fu and C.-W. Shu, Analysis of an embedded discontinuous Galerkin method with implicitexplicit time-marching for convection-diffusion problems, Int. J. Numer. Anal. Model., 347 (2017), pp. 305–327.
- C. A. KENNEDY AND M.-H. CARPENTER, Additive Runge-Kutta schemes for convectiondiffusion-reaction equations, Appl. Numer. Math., 44 (2003), pp. 139–181.
- S. ORTLEB, L²-stability analysis of IMEX-(σ, μ)DG schemes for linear advection-diffusion equations, Appl. Numer. Math., 147 (2020), pp. 43–65.
- Z.C. Peng, Y.D. Ying, J.M. Qiu and F.Y. Li, Stability-enhanced AP IMEX-LDG schemes for linear kinetic transport equations under a diffusive scaling, J. Comput. Phys., 415 (2020), 109485.
- M. A. REYNA AND F. LI, Operator bounds and time step conditions for DG and central DG methods, J. Sci. Comput., 62 (2015), pp. 532–554.
- H. J. Wang, C.-W. Shu and Q. Zhang, Stability and error estimates of local discontinuous Galerkin methods with implicit-explicit time-marching for advection-diffusion problems, SIAM J. Numer. Anal., 53 (2015), pp. 206-227.
- H. J. Wang, C.-W. Shu and Q. Zhang, Stability analysis and error estimates of local discontinuous Galerkin methods with implicit-explicit time-marching for nonlinear convectiondiffusion problems, Appl. Math. Comput., 272 (2016), pp. 237–258.
- 13. H. J. Wang and Q. Zhang, The direct discontinuous Galerkin methods with implicit-explicit Runge-Kutta time marching for linear convection-diffusion problems, Communications on Applied Mathematics and Computation, 4 (2022), pp. 271–292.
- 14. H. J. Wang, Q. Zhang, S. P. Wang and C.-W. Shu, Local discontinuous Galerkin methods with explicit-implicit-null time discretizations for solving nonlinear diffusion problems, Sci. China Math., 63 (2020), pp. 183–204.
- 15. Y. Xu and C.-W. Shu, Local discontinuous Galerkin methods for high-order time-dependent partial differential equations, Commun. Comput. Phys., 7 (2010), pp. 1–46.
- Y. Xu, C.-W. Shu and Q. Zhang, Error estimate of the fourth order Runge-Kutta discontinuous Galerkin methods for linear hyperbolic equations, SIAM J. Numer. Anal, 58 (2020), pp. 2885–2914.
- Y. Xu, Q. Zhang, C. -W. Shu and H. J. Wang, The L²-norm stability analysis of Runge-Kutta discontinuous Galerkin methods for linear hyperbolic equations, SIAM J. Numer. Anal, 57 (2019), pp. 1574–1601.
- Q. ZHANG AND F. Z. GAO, A fully-discrete local discontinuous Galerkin method for convectiondominated Sobolev equation, J. Sci. Comput., 51 (2012), pp. 107–134.
- 19. Q. Zhang and C. -W. Shu, Error estimates to smooth solution of Runge-Kutta discontinuous Galerkin methods for scalar conservation laws, SIAM J. Numer. Anal., 42 (2004), pp. 641–666.

School of Science, Nanjing University of Posts and Telecommunications, Nanjing 210023, Jiangsu Province, People's Republic of China

Email address: hjwang@njupt.edu.cn

Department of Mathematical Sciences, Rensselaer Polytechnic Institute, Troy, New York 12180

 $Email\ address: \ {\tt lif@rpi.edu}$

Division of Applied Mathematics, Brown University, Providence, Rhode Island 02912 $\it Email\ address$: chi-wang_shu@brown.edu

CORRESPONDING AUTHOR. DEPARTMENT OF MATHEMATICS, NANJING UNIVERSITY, NANJING 210093, JIANGSU PROVINCE, PEOPLE'S REPUBLIC OF CHINA

Email address: qzh@nju.edu.cn